ENTE PER LE NUOVE TECNOLOGIE,
L'ENERGIA E L'AMBIENTE

Dipartimento Ambiente

AIR KERMA TO PERSONAL DOSE EQUIVALENT CONVERSION FACTORS FOR THE ICRU AND ISO RECOMMENDED SLAB PHANTOMS FOR PHOTONS FROM 20 keV TO 1 MeV

G.F. GUALDRINI, B. MORELLI
ENEA - Centro Ricerche "Ezio Clementel", Bologna

RT/AMB/96/15

Testo pervenuto nel settembre 1996

SUMMARY

The present report summarises the studies carried out at ENEA-AMB-PRO-IRP (Institute for Radiation Protection) that were addressed to the determination of air kerma to personal dose equivalent conversion coefficients for two practical phantoms as proposed by ICRU (International Commission for Radiation Units and Measurements) and by ISO (International Standard Organization) for photon personal dosemeters' calibration procedure.
The analyses, developped using the MCNP Monte Carlo code, were mainly aimed at establishing which of the two proposed phantoms better approximates the ICRU theoretical one. Furthermore a complete tabulation of the conversion coefficients is supplied for monoenergetic photon beams from 20 keV to 1 MeV as well as for the two ISO X-ray reference series Wide Spectrum and Narrow Spectrum.

The study has been performed in the framework of the CEC Contract F13P-CT92-0064 "The Measurement of the Spectral and Angular Distribution of External Radiations in Workplace and Implications for Personal Dosimetry."

keywords: ISO X-RAY BEAMS, AIR KERMA TO PERSONAL DOSE EQUIVALENT CONVERSION FACTORS, CALIBRATION PHANTOMS, ICRU TISSUE SUBSTITUTE MATERIALS, MONTE CARLO METHOD.

RIASSUNTO

Il presente rapporto sintetizza gli studi svolti presso l'ENEA-AMB-PRO-IRP (Istituto per la Radioprotezione) riguardanti la determinazione dei coefficienti di conversione fra kerma in aria libera ed equivalente di dose personale a diverse profondità per due tipi di fantocci pratici consigliati da ICRU (International Commission for Radiation Units and Measurements) e da ISO (International Standard Organization) per la calibrazione dei dosimetri personali per fotoni.
Le analisi, svolte mediante il codice Monte Carlo MCNP, hanno avuto il principale scopo di stabilire quale dei dei due fantocci pratici proposti meglio approssimi il riferimento teorico ICRU e di fornire una tabulazione completa dei suddetti fattori per energie di fotoni monocromatici da 20 keV a 1 MeV e per le due serie ISO di fasci X di riferimento Wide Spectrum e Narrow Spectrum.

Lo studio è stato svolto nell'ambito del Contratto CEC F13P-CT92-0064 "The Measurement of the Spectral and Angular Distribution of External Radiations in Workplace and Implications for Personal Dosimetry."

parole chiave: FASCI DI RAGGI X ISO, FATTORI DI CONVERSIONE FRA KERMA IN ARIA ED EQUIVALENTE DI DOSE PERSONALE, FANTOCCI DI CALIBRAZIONE, MATERIALI SOSTITUTIVI DEL TESSUTO ICRU, METODO MONTE CARLO.

INDEX

1. INTRODUCTION

Some years ago ICRU Publication 39 /1/, recommended, for personal dosemeter calibration purposes, the two operational quantities individual dose equivalent superficial (Hs(d)) and penetrating (Hp(d)).

These two quantities were defined as the dose equivalent in soft tissue at a depth *d* below a specified point on the body.

The personal dosemeters, normally worn on the human trunk, had therefore to be calibrated in terms of Hp(d) or Hs(d), depending on the radiation quality.

In the same publication the ICRU recommended the ICRU sphere (a theoretical 30 cm diameter sphere with specific gravity of 1 g/cm^3 and mass composition of 76.2% Oxygen, 11.1% Carbon, 10.1% Hydrogen and 2.6% Nitrogen) as a suitable phantom for calibration purposes[1].

A series of criticisms, especially practical but also theoretical, were formulated against the choice of the ICRU sphere as calibration phantom. One of the theoretical aspects was related to the so-called "ears effect" that generated dose maxima in the sphere towards 90° from the radiation incident direction. This effect that was experienced at higher energies due to the forward peaked incoherent scattering coupled with the spherical shape of the phantom, was completely non physical for the human trunk that is in reality more similar to an elliptic cylinder. A further practical criticism was based on the impossibility of contemporary calibration of several dosemeters at the same time. The spherical shape in fact allows only one dosemeter to be calibrated during an irradiation. Moreover, from the manufacturing point of view, the ICRU sphere is not easy to be provided whilst slab phantoms are very easy to be built and allow contemporary calibration of a number of personal dosemeters. As far as this last point is concerned, a series of numerical analyses have been carried out /7/ to state the limits of

---

[1] Several investigation have been carried out in the past at ENEA-AMB-IRP on the ICRU sphere that have been documented both in the open literature and in four ENEA reports /2/ /3/ /4/ /5/ /6/.

the area on the front face of the calibration slab, where the irradiation conditions could be assumed as homogeneous.
Following the mentioned series of criticisms the more recent ICRU Publications /8/ /9/, based on the concept of personal dose equivalent Hp(d) for individual monitoring (defined in the same way as previous individual dose equivalent), suggested a PMMA 30x30x15 slab phantom, whilst more recently ISO /10/ indicated an equal dimension water phantom with PMMA walls of 10 mm thickness except for the wall facing the source that is 2 mm thick. The operational quantity Hp(d) is defined in a phantom with the same composition of the theoretical ICRU material, of the same shape and dimensions of the practical phantom used in the calibration procedure. It should be therefore necessary, besides applying the conversion factors Hp/ka for the theoretical ICRU slab phantom (where ka is the air kerma that is the quantity directly related to exposure in which terms dosemeters were calibrated until now in Italy), to apply correction factors taking into account the different backscattering properties of the practical phantom employed for calibration.

A simpler solution to the problem could be to use operational quantities directly defined on the employed phantom.
An extensive numerical study has been therefore carried out on the two practical phantoms, specifically aimed at evaluating which of the two is a better substitute of the theoretical ICRU one.
The investigated depths were 0.07 mm (for the first sensible skin layer), 3 mm (for the eye lens) and finally 10 mm (for the deep organs). Some calculations were also performed for 0.1 mm depth to compare the results with those supplied by other authors /11/.

2. MONTE CARLO CALCULATIONS

2.1 Numerical procedure

The numerical evaluation was performed simulating the photon transport by means of the Monte Carlo code MCNP /12/. The code, that makes use of photon interaction data taken from Hubbell /13/, can describe highly complex geometries and is endowed with a large variety of variance reduction techniques, allowing to obtain low second moment values (σ^2) in reasonable CPU time. The photon transport has been followed in the so-called "detailed physics" approach that is not very crucial to be used for the light materials involved in the present problem. This approach takes into account the fluorescent emission and the modification of the Thomson and Klein-Nishina differential cross section through appropriate form factors to take into account binding effects.
The irradiation experience (see Fig. 1) was simplified neglecting the air presence. Furthermore, the various calculations have been carried out in the so-called kerma approximation, neglecting the secondary electron transport. A condition of secondary charged particle equilibrium (electrons and positrons) has therefore to be fulfilled. This condition is dependent both on the secondary electron range in air and in the tissue equivalent material under study (e.g. source to phantom distance and depth in the phantom where the dose equivalent is calculated). As far as the present study is concerned, the secondary electron range in air for the maximum treated

energy (1 MeV photons) is about 3 m, corresponding to the practical distance between source and phantom employed at the Secondary Standard Dosimetry Laboratory of IRP.

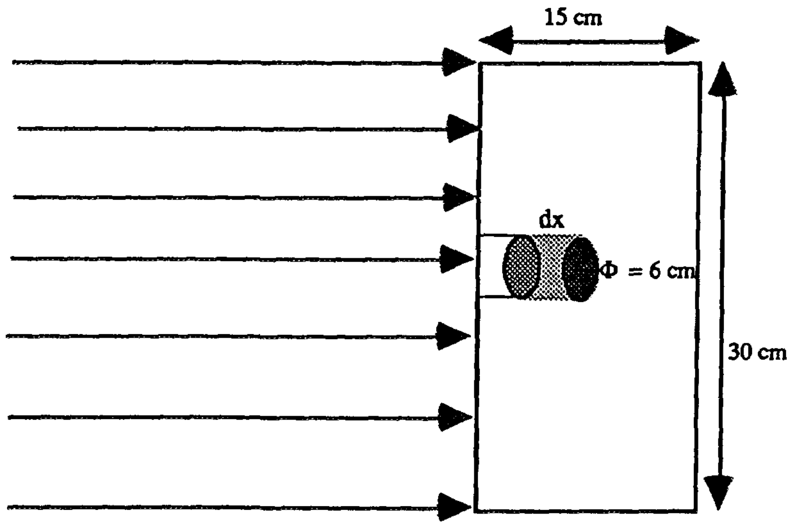

Fig. 1: Irradiation experiment layout (the scoring volume inside the phantom for fluence tracklength estimator is shown).

In addition, 1 MeV photons generate secondary electrons with maximum range of about 4 mm in soft tissue, that guarantees that electronic equilibrium is attained at 10 mm,, the suitable depth for penetrating radiations. The kerma approximation was therefore taken as a sufficient approach.
The incident photon beams have been considered as homogeneous, aligned and expanded on a volume completely including the slab phantom. For each run a sample of 10^6 particles have been analysed, that allowed to obtain uncertainties on the results within 1% and 1.5% (1 σ).

2.2 Personal dose equivalent calculation

The conversion coefficient linking the receptor-free collision air kerma (ka) and the personal dose equivalent Hp(d) at a depth d below the phantom surface, on its principal axis, is given by:

$$h(d) = H_p(d)/ka$$

where $ka = \phi_0 E_0 [\mu_{en}(E_0)/\rho]_{air}$ and

$$H_p(d) = \int_0^\infty (d\phi/dE)_d E [\mu_{en}(E)/\rho]_{icru} \, dE$$

In the previous expression $(d\phi/dE)_d$ is the photon spectral fluence at the depth *d* within the energy range E - E+dE and $[\mu_{en}(E)/\rho]_{icru}$ is the mass energy absorption coefficient for the theoretical ICRU tissue to which the definition of Hp(d) is referred according to the ICRU document 47.

The following three phantoms were analysed:

- ICRU four element theoretical 30x30x15 cm slab phantom (specific gravity 1.0 g/cm^3);

- PMMA 30x30x15 cm slab phantom as suggested by ICRU (specific gravity 1.19 g/cm^3);

- Water with PMMA walls 30x30x15 cm slab phantom as suggested by ISO (bulk of the phantom specific gravity 1.0 g/cm^3).

For the mentioned three phantoms the conversion coefficients Hp(d)/ka have been calculated at the three depths recommended by ICRU (0.07, 3 and 10 mm) with the addition of 0.1 mm depth.

To supply a preliminary idea of the variations of Hp(d) when adopting a slab phantom instead of the previously proposed ICRU sphere, the results at the three investigated depths for the theoretical ICRU sphere and for the ICRU 30x30x15 slab were compared. Figures 2, 3 and 4 show the mentioned comparison, demonstrating the higher response for the slab in spite of its smaller mass. The slab shape implies an higher contribution to the response from scattered radiation coming from the regions placed on the lateral side of the scoring volume. Tissue material at the same position is obviously missing within the sphere so that a lower scattered contribution is expected.

Fig. 2: Hp(0.07)/ka comparison between ICRU sphere and ICRU slab.

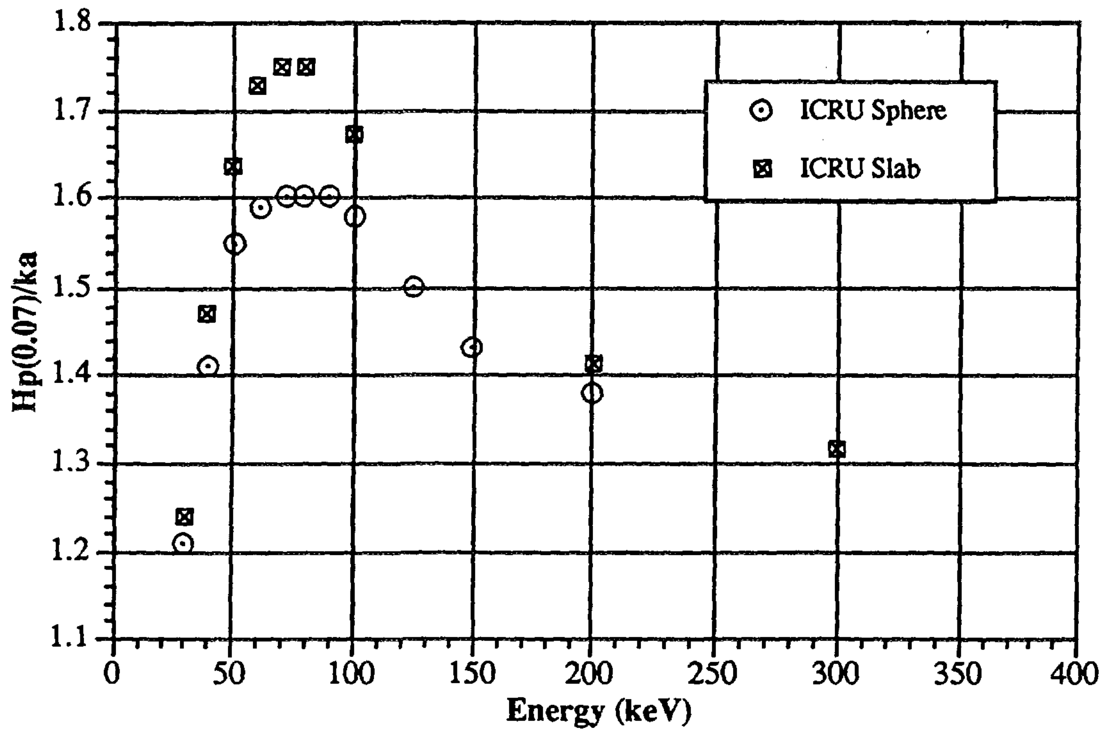

Fig. 3: Hp(3)/ka comparison between ICRU sphere and ICRU slab.

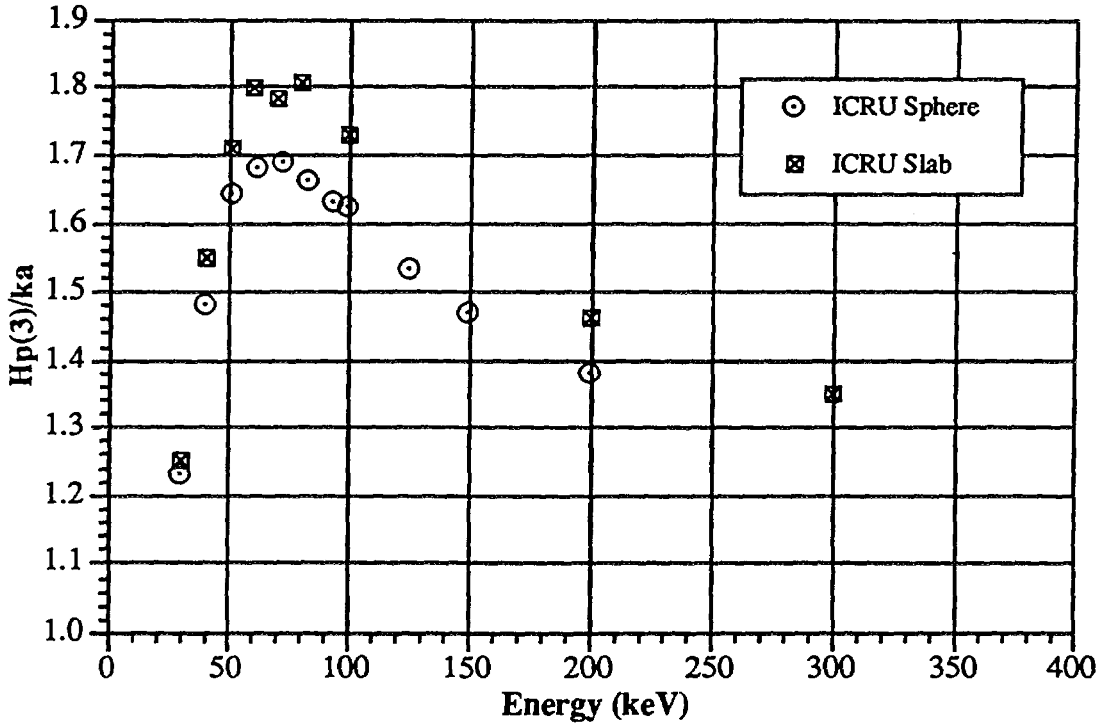

Fig. 4: Hp(10)/ka comparison between ICRU sphere and ICRU slab.

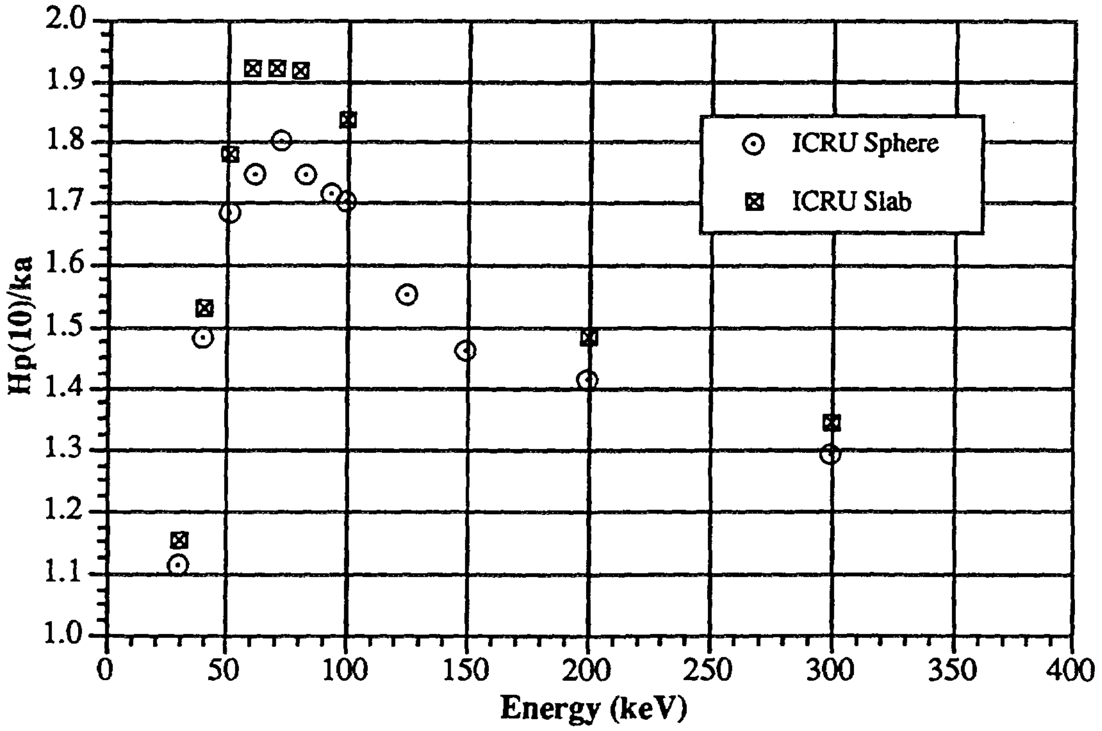

A first series of calculations dealt with monoenergetic photon beams with energies ranging from 20 keV to 1 MeV.
In a second set of calculations two reference ISO Series were treated (Wide Spectrum and Narrow Spectrum). The first one is the X-ray series commonly used at ENEA-IRP Secondary Standard Dosimetry Laboratory, due to its high air kerma rate that has to be ascribed to the low filtration of the beams. The second one is the series recommended by ISO for the routine calibration procedures. It is characterised by a rather low air kerma rate, so that longer irradiation times are necessary to achieve the same level of precision as using the Wide Spectrum Series.

The spectral fluence was determined by Monte Carlo simulation using a "volume tracklength estimator". The scoring volume, as shown in Fig. 1, consists of a cylinder with 3 cm radius basis and the height of the order of a few thousandths of the investigated depth, that allowed to neglect the fluence variation, due to attenuation, as a function of depth within the scoring volume.

As far as the oblique incidence of the photon beams is concerned, a set of conversion coefficients for PMMA slab was produced for the Wide and Narrow Spectrum Series at 45°, 60° and 75° incident angles.

3. RESULTS

3.1 Monoenergetic photons

Tables I-IV summarise the values of the conversion coefficients Hp(d)/ka computed for monoenergetic photon beams with energies ranging from 20 keV to 1 MeV for the three investigated phantoms at the depth 0.07 mm, 0.1 mm, 3 mm and finally 10 mm. In the same tables the values obtained by Grosswendt are supplied only for ICRU theoretical slab and PMMA slab.

Tab. I: Hp(0.07)/ka for the three slabs.

Eγ	ICRU			PMMA		water in PMMA	
(keV)	fract mfp *	ENEA	PTB	fract mfp *	ENEA	fract mfp *	ENEA
20	5.4E-3	1.065	1.040	4.8E-3	1.122	4.8E-3	1.079
30	2.5E-3	1.238	1.227	2.5E-3	1.366	2.5E-3	1.272
40	1.8E-3	1.469	1.441	2.0E-3	1.641	2.0E-3	1.474
50	1.6E-3	1.635	1.629	1.7E-3	1.817	1.7E-3	1.653
60	1.4E-3	1.725	1.720	1.6E-3	1.877	1.6E-3	1.758
70	1.3E-3	1.746	1.741	1.2E-3	1.932	1.2E-3	1.761
80	1.3E-3	1.748	1.719	1.5E-3	1.869	1.5E-3	1.758
100	1.2E-3	1.670	1.670	1.4E-3	1.788	1.4E-3	1.681
200	9.5E-4	1.412	1.424	1.1E-3	1.482	1.1E-3	1.441
300	8.2E-4	1.314	1.338	9.6E-4	1.355	9.6E-4	1.336
1000	4.9E-4	1.169	1.179	5.7E-4	1.185	5.7E-4	1.173

Tab. II: Hp(0.1)/ka for the two practical slabs.

Energy	PMMA			water in PMMA	
(keV)	fract mfp *	ENEA	PTB	fract mfp *	ENEA
20	6.8E-3	1.120	1.087	6.8E-3	1.080
30	3.6E-3	1.376	1.323	3.6E-3	1.258
40	2.8E-3	1.613	1.577	2.8E-3	1.477
50	2.5E-3	1.817	1.759	2.5E-3	1.674
60	2.3E-3	1.929	1.848	2.3E-3	1.758
70	1.8E-3	1.878	1.859	1.8E-3	1.763
80	2.1E-3	1.864	1.831	2.1E-3	1.764
100	2.0E-3	1.766	1.746	2.0E-3	1.685
200	1.6E-3	1.464	1.460	1.6E-3	1.445
300	1.4E-3	1.345	1.359	1.4E-3	1.335
1000	8.2E-4	1.182	1.179	8.2E-4	1.178

(*) mean free path percentage corresponding to the investigated depth (for the water filled PMMA phantom the values are referred to PMMA at 0.07 mm and 0.1 mm depth whilst for the other two depths are those referred to pure water).

Tab. III: Hp(3)/ka for the three slabs.

Eγ	ICRU			PMMA			water in PMMA	
(keV)	fract mfp *	ENEA	PTB	fract mfp *	ENEA	PTB	fract mfp *	ENEA
20	2.3E-1	0.939	0.909	2.0E-1	1.061	0.984	2.4E-1	0.959
30	1.1E-1	1.250	1.223	1.1E-1	1.398	1.348	1.1E-1	1.252
40	7.8E-2	1.545	1.496	8.4E-2	1.707	1.657	8.0E-2	1.523
50	6.7E-2	1.707	1.713	7.4E-2	1.934	1.880	6.8E-2	1.718
60	6.1E-2	1.796	1.807	6.9E-2	2.010	1.976	6.2E-2	1.864
70	5.8E-2	1.783	1.823	5.3E-2	1.981	1.994	5.8E-2	1.855
80	5.4E-2	1.805	1.809	6.3E-2	1.968	1.941	5.5E-2	1.812
100	5.1E-2	1.726	1.743	5.9E-2	1.842	1.831	5.1E-2	1.740
200	4.1E-2	1.460	1.463	4.7E-2	1.527	1.499	4.1E-2	1.474
300	3.5E-2	1.347	1.354	4.1E-2	1.394	1.383	3.6E-2	1.367
1000	2.1E-2	1.164	1.182	2.5E-2	1.180	1.184	2.1E-2	1.176

Tab. IV: Hp(10)/ka for the three slabs.

Eγ	ICRU			PMMA			water in PMMA	
(keV)	fract mfp *	ENEA	PTB	fract mfp *	ENEA	PTB	fract mfp *	ENEA
20	7.6E-1	0.644	0.613	6.8E-1	0.758	0.718	8.1E-1	0.631
30	3.6E-1	1.155	1.105	3.6E-1	1.346	1.254	3.8E-1	1.129
40	2.6E-1	1.529	1.495	2.8E-1	1.742	1.683	2.7E-1	1.516
50	2.2E-1	1.778	1.769	2.5E-1	1.982	1.979	2.3E-1	1.783
60	2.0E-1	1.921	1.890	2.3E-1	2.110	2.095	2.1E-1	1.949
70	1.9E-1	1.921	1.911	1.8E-1	2.105	2.109	1.9E-1	1.956
80	1.8E-1	1.916	1.891	2.1E-1	2.100	2.051	1.8E-1	1.943
100	1.7E-1	1.832	1.812	2.0E-1	1.978	1.926	1.7E-1	1.831
200	1.4E-1	1.483	1.489	1.6E-1	1.543	1.531	1.4E-1	1.495
300	1.2E-1	1.342	1.370	1.4E-1	1.403	1.396	1.2E-1	1.369
1000	7.0E-2	1.167	1.175	8.2E-2	1.174	1.177	7.1E-2	1.176

Figures 5, 6 and 7 show the comparison of the conversion coefficients for the ICRU theoretical slab with the values calculated by Grosswendt.

A satisfactory agreement has to be pointed out. The agreement is within 2 - 3% for the three depths with an overestimation of the ENEA results of about 4-5% at 20-30 keV for 10 mm depth.

Fig. 5-6-7: Comparison of Hp(d)/Ka for the ICRU theoretical slab.

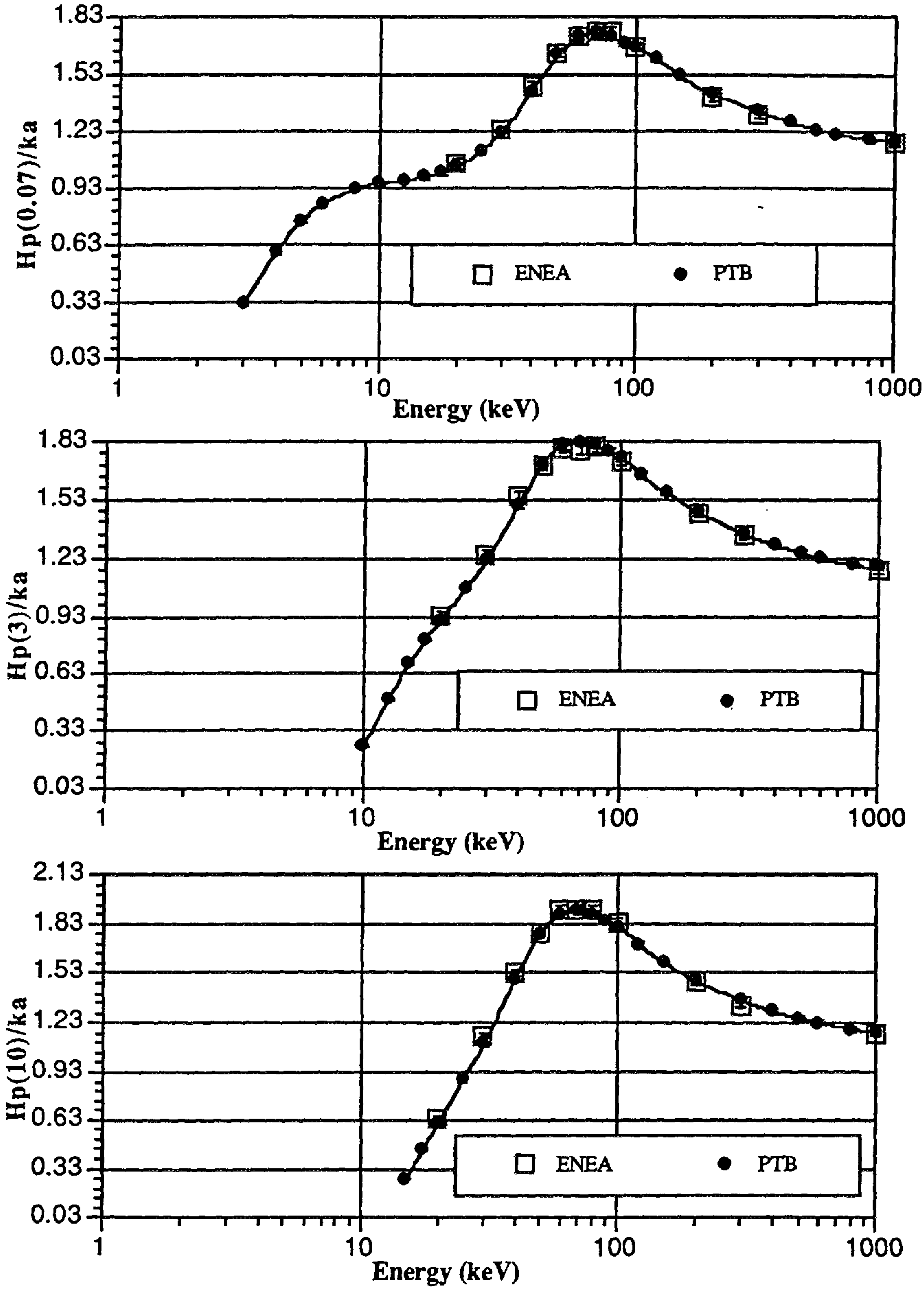

Similar conclusions can be drawn for the PMMA slab phantom, with a systematic trend to overestimate for the ENEA results if compared with the Grosswendt's ones especially at lower energies (see figures 8 , 9 and 10).

Fig. 8: Hp(0.1)/ka comparison with data by Grosswendt for the PMMA slab.

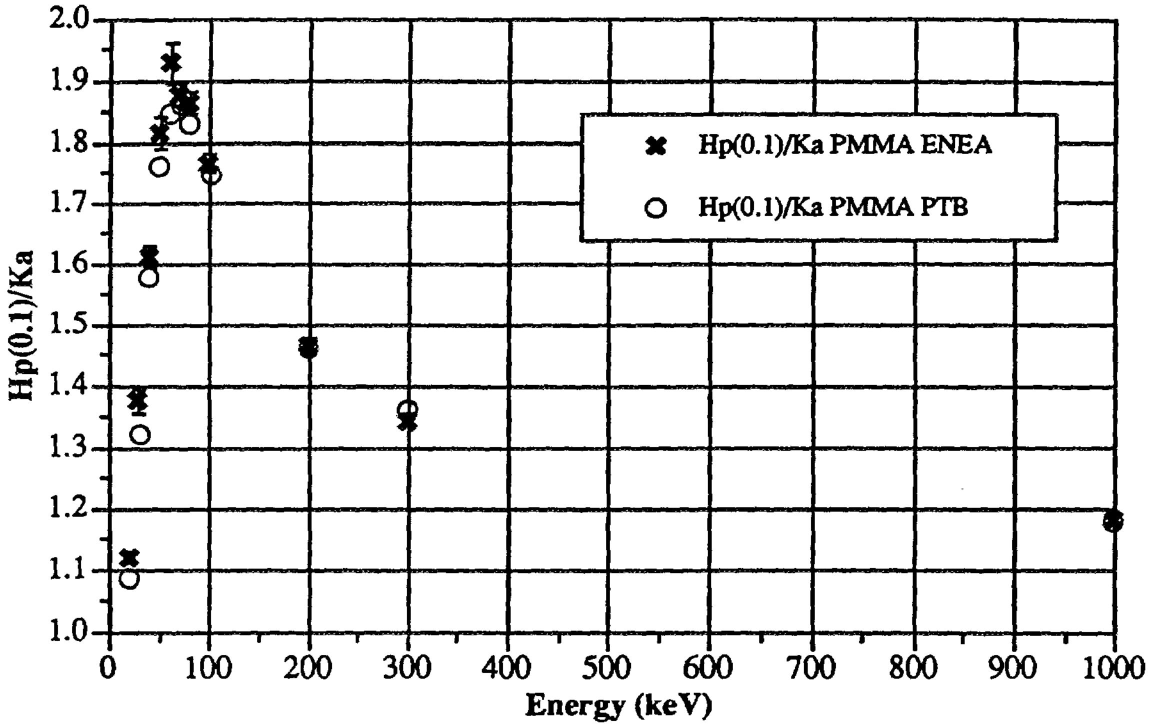

Fig. 9: Hp(3)/ka comparison with data by Grosswendt for the PMMA slab.

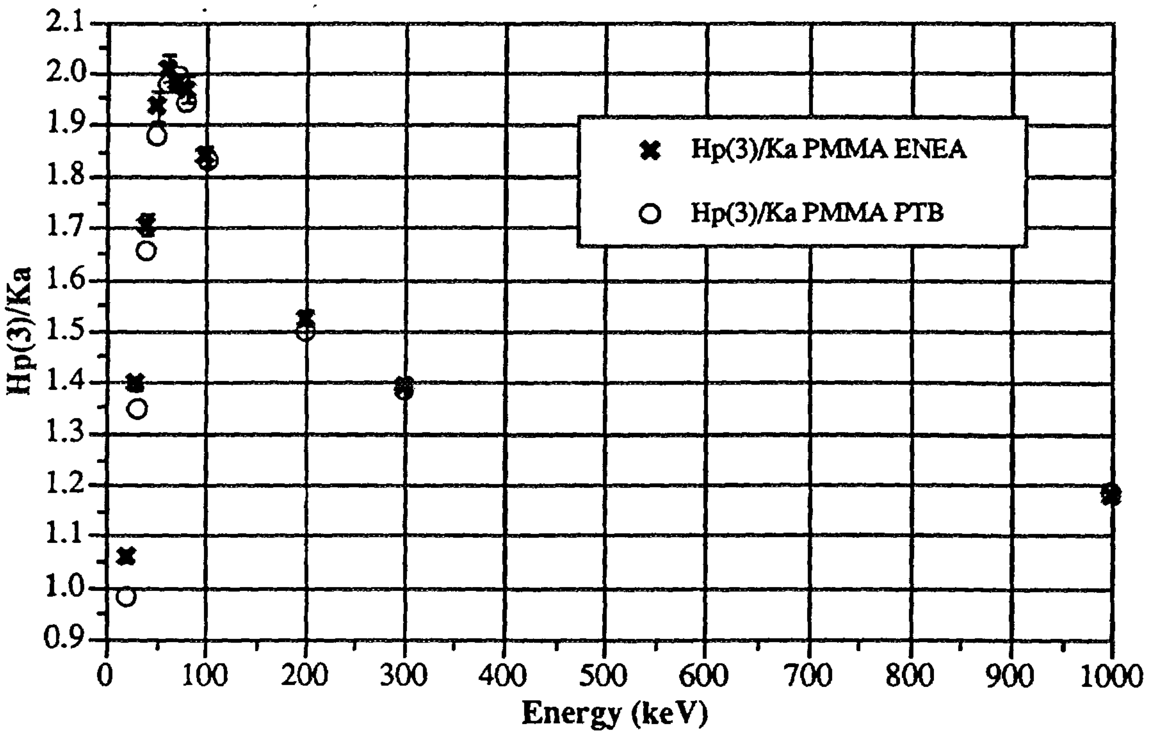

Fig. 10: Hp(10)/ka comparison with data by Grosswendt for the PMMA slab.

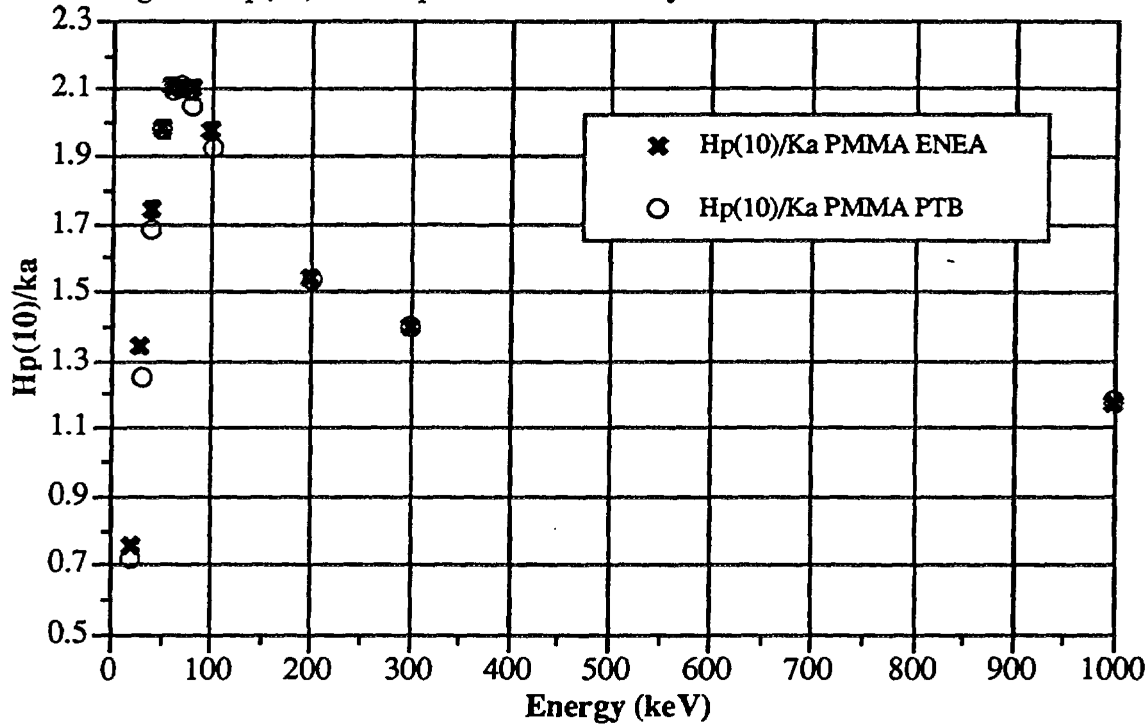

Finally the results obtained for monoenergetic beams have been employed to compare the air kerma to personal dose equivalent conversion coefficients for the two investigated practical phantoms with the values calculated for the theoretical ICRU slab phantom.

The results are reported in figures 11, 12 and 13.

Fig. 11: Comparison of Hp/ka conversion coefficients in the three materials.

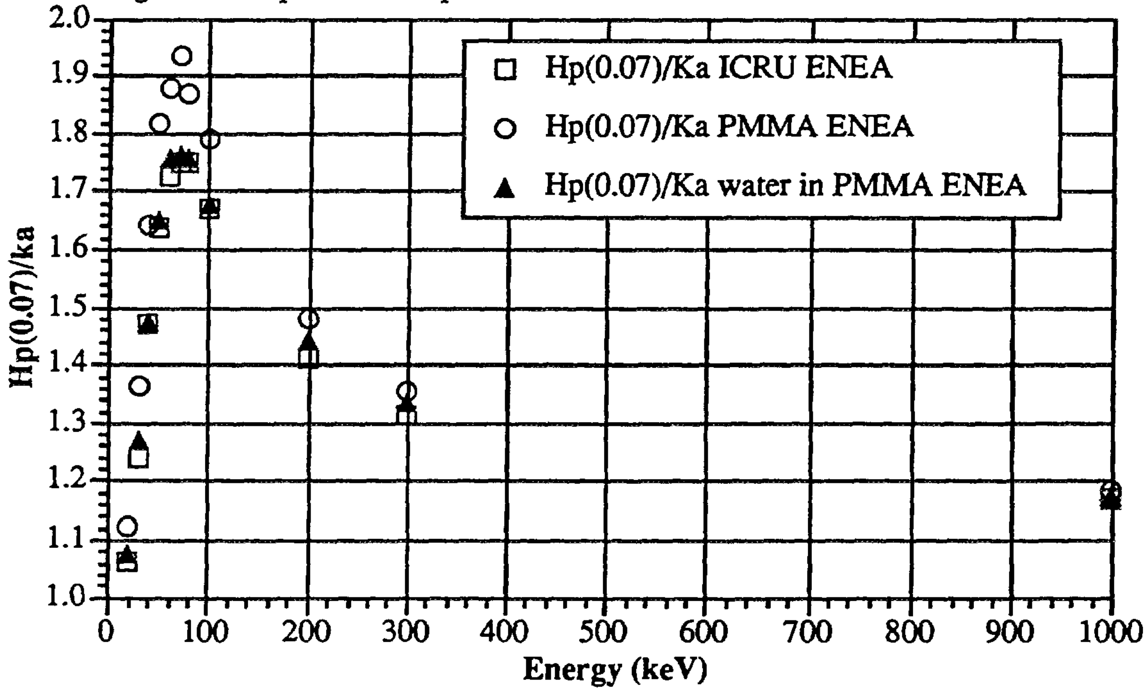

Fig. 12: Comparison of Hp/ka conversion coefficients in the three materials.

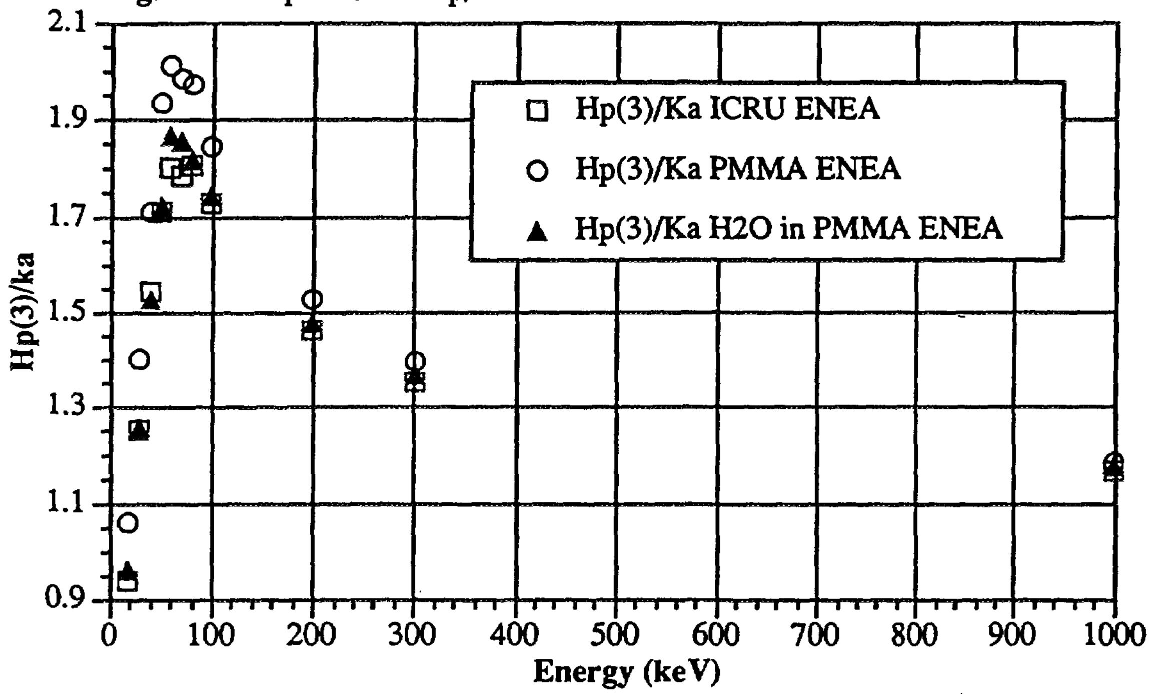

Fig. 13: Comparison of Hp/ka conversion coefficients in the three materials.

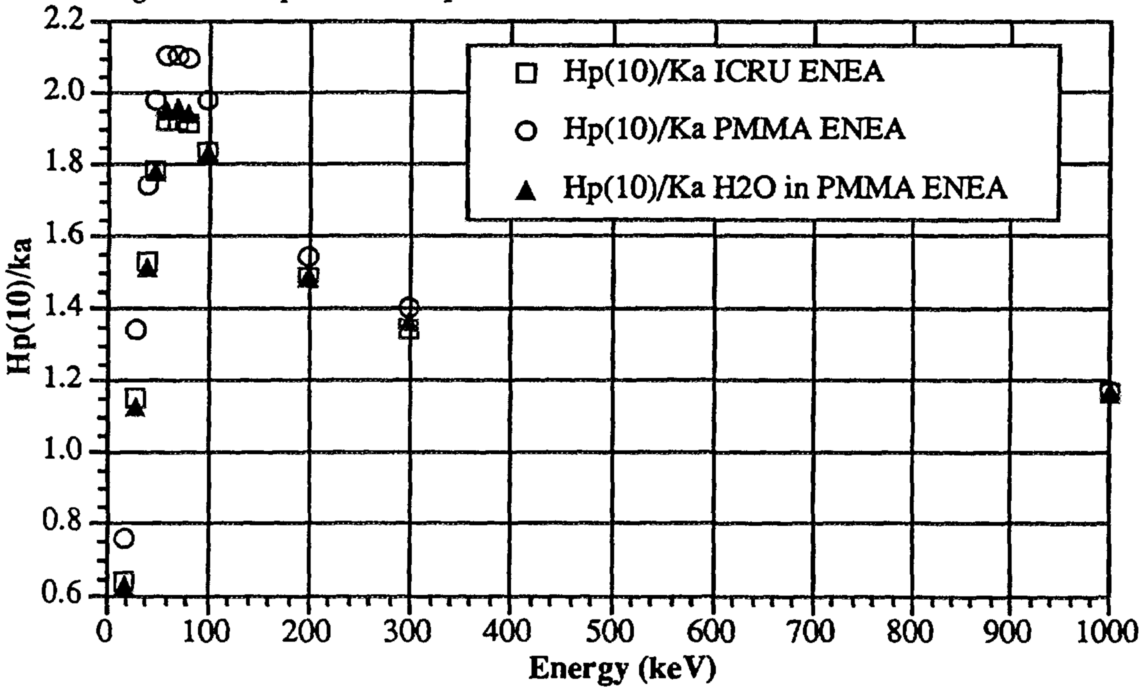

The results at 0.07 mm depth can be taken as representative of the collision air kerma backscatter factor (taking into account the ratio of air and ICRU tissue μ_{en}/ρ). It has to be pointed out that the energy deposition at this depth is governed by the backscattering characteristics of the bulk of the phantom. This is the reason why the response in the water filled PMMA slab (that is scored within the 2 mm thick PMMA wall) is closer to that of the ICRU theoretical material than to the response in the pure PMMA slab.

At the three investigated depths higher Hp(d) values have been obtained, as expected, for the pure PMMA slab if compared with the calculated values for water filled PMMA phantom. The deviations are within 5% - 11% with the maxima placed around 50 - 70 keV where the conversion coefficients are reaching their highest values. On the other hand the water filled PMMA phantom as proposed by ISO presents a very satisfactory agreement with the Hp(d) values of the ICRU theoretical one. The agreement is within 1% - 2.5%, that could qualitatively be foreseen also from the analysis of the respective linear attenuation coefficients.
The study allowed therefore to conclude that the water filled PMMA phantom is a better substitute for the ICRU theoretical one.

3.2 Wide and Narrow Spectrum ISO reference beams

As mentioned before the routinely used X-ray ISO reference series at the ENEA-IRP Secondary Standard Dosimetry Laboratory is the Wide Spectrum Series due to its high air kerma rate.
A series of calculations with practical calibration spectra /14/ have been therefore carried out to complete the study. Besides the Wide Spectrum Series, the Narrow Spectrum Series was also studied being the ISO recommended one for the photon personal dosemeters' calibration procedure.
The investigations were concerned both with the normal incidence beams and with the oblique incidence beams (at 45°, 60° and 75° only for the PMMA phantom).

3.2-A Normal incidence beams

The complete Wide and Narrow Series spectra were supplied to MCNP for sampling the source energy distributions. A set of 10^6 photons was followed for each run as for the monoenergetic photons.
In Tab. V, VI, VII and VIII the complete set of the results for normally incident beams is shown at 0.07, 0.1, 3 and 10 mm depths in the PMMA phantom.

Tab. V: Hp(0.07,0°)/ka values for PMMA slab phantom.

Depth =0.07 mm Hp(d;0°)/ka					
PMMA					
Wide Spectrum Series			Narrow Spectrum Series		
Spectrum	ENEA	PTB	Spectrum	ENEA	PTB
L1 - 60 kV	1.678	1.656	S1 - 40 kV	1.395	1.405
L2 - 80 kV	1.816	1.789	S2 - 60 kV	1.741	1.705
L3 - 110 kV	1.829	1.817	S3 - 80 kV	1.861	1.854
L4 - 150 kV	1.698	1.728	S4 - 100 kV	1.832	1.812
L5 - 200 kV	1.588	1.613	S5 - 120 kV	1.775	1.740
L6 - 250 kV	1.534	1.515	S6 - 150 kV	1.643	1.677
L7 - 300 kV	1.478	1.455	S7 - 200 kV	1.557	1.526
			S8 - 250 kV	1.462	1.446
			S9 - 300 kV	1.417	1.397

Tab. VI: Hp(0.1,0°)/ka values for PMMA slab phantom.

Depth =0.1 mm Hp(d;0°)/ka			
PMMA			
Wide Spectrum Series		Narrow Spectrum Series	
Spectrum	ENEA	Spectrum	ENEA
L1 - 60 kV	1.681	S1 - 40 kV	1.395
L2 - 80 kV	1.813	S2 - 60 kV	1.814
L3 - 110 kV	1.984	S3 - 80 kV	1.851
L4 - 150 kV	1.700	S4 - 100 kV	1.842
L5 - 200 kV	1.592	S5 - 120 kV	1.774
L6 - 250 kV	1.536	S6 - 150 kV	1.643
L7 - 300 kV	1.480	S7 - 200 kV	1.557
		S8 - 250 kV	1.464
		S9 - 300 kV	1.417

Tab. VII: Hp(3,0°)/ka values for PMMA slab phantom.

Depth =3 mm Hp(d;0°)/ka					
PMMA					
Wide Spectrum Series			Narrow Spectrum Series		
Spectrum	ENEA	PTB	Spectrum	ENEA	PTB
L1 - 60 kV	1.742	1.731	S1 - 40 kV	1.441	1.423
L2 - 80 kV	1.916	1.887	S2 - 60 kV	1.848	1.792
L3 - 110 kV	1.954	1.914	S3 - 80 kV	1.972	1.955
L4 - 150 kV	1.798	1.805	S4 - 100 kV	1.939	1.911
L5 - 200 kV	1.659	1.676	S5 - 120 kV	1.816	1.818
L6 - 250 kV	1.565	1.572	S6 - 150 kV	1.756	1.745
L7 - 300 kV	1.501	1.508	S7 - 200 kV	1.587	1.584
			S8 - 250 kV	1.507	1.500
			S9 - 300 kV	1.468	1.443

Tab. VIII: Hp(10,0°)/ka values for PMMA slab phantom.

Depth =10 mm Hp(d;0°)/ka					
PMMA					
Wide Spectrum Series			*Narrow Spectrum Series*		
Spectrum	ENEA	PTB	Spectrum	ENEA	PTB
L1 - 60 kV	1.837	1.795	S1 - 40 kV	1.421	1.372
L2 - 80 kV	2.028	2.000	S2 - 60 kV	1.972	1.874
L3 - 110 kV	2.076	2.041	S3 - 80 kV	2.114	2.095
L4 - 150 kV	1.876	1.905	S4 - 100 kV	2.058	2.034
L5 - 200 kV	1.745	1.759	S5 - 120 kV	1.937	1.919
L6 - 250 kV	1.630	1.625	S6 - 150 kV	1.778	1.831
L7 - 300 kV	1.547	1.538	S7 - 200 kV	1.633	1.654
			S8 - 250 kV	1.520	1.520
			S9 - 300 kV	1.495	1.449

Fig. 14-19 supply the comparisons with the values calculated by Grosswendt for the same phantom. Taking into account the different spectral distributions employed in two sets of calculations, a satisfactory agreement has to be pointed out.

Fig. 14: Wide Spectrum Series: Hp(0.07,0°)/ka for PMMA slab phantom.

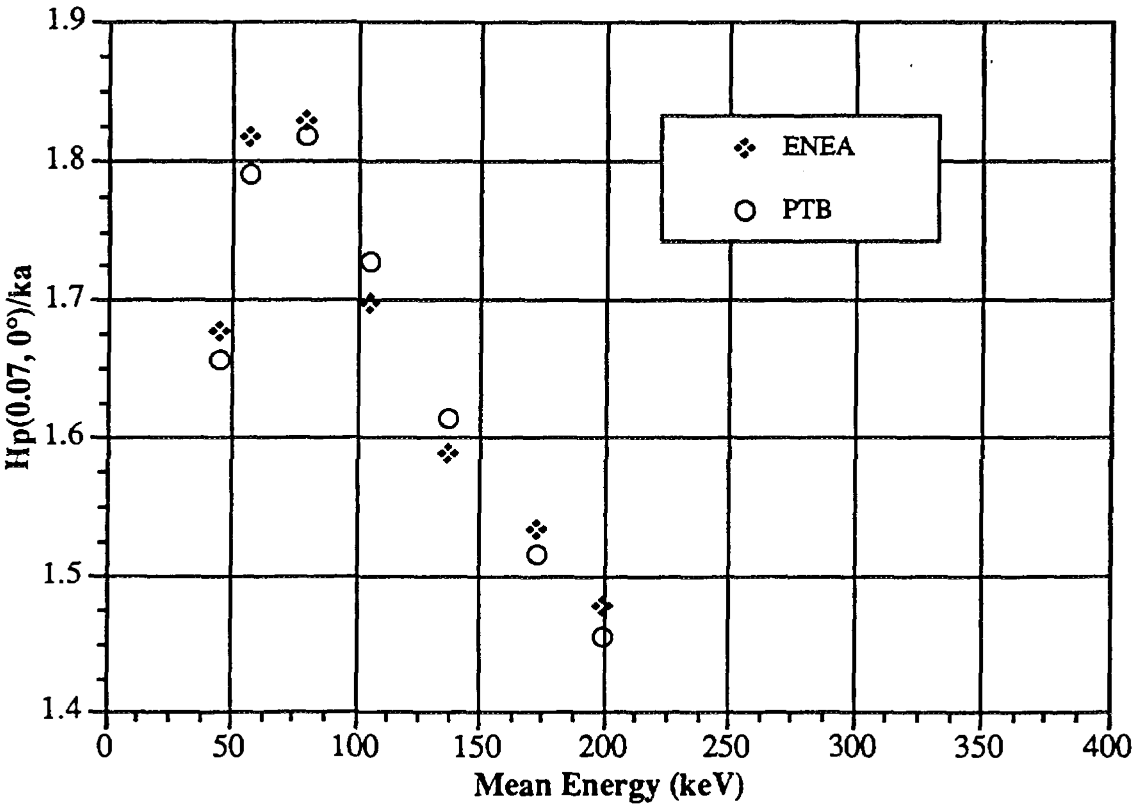

Fig. 15: Wide Spectrum Series: Hp(3,0°)/ka for PMMA slab phantom.

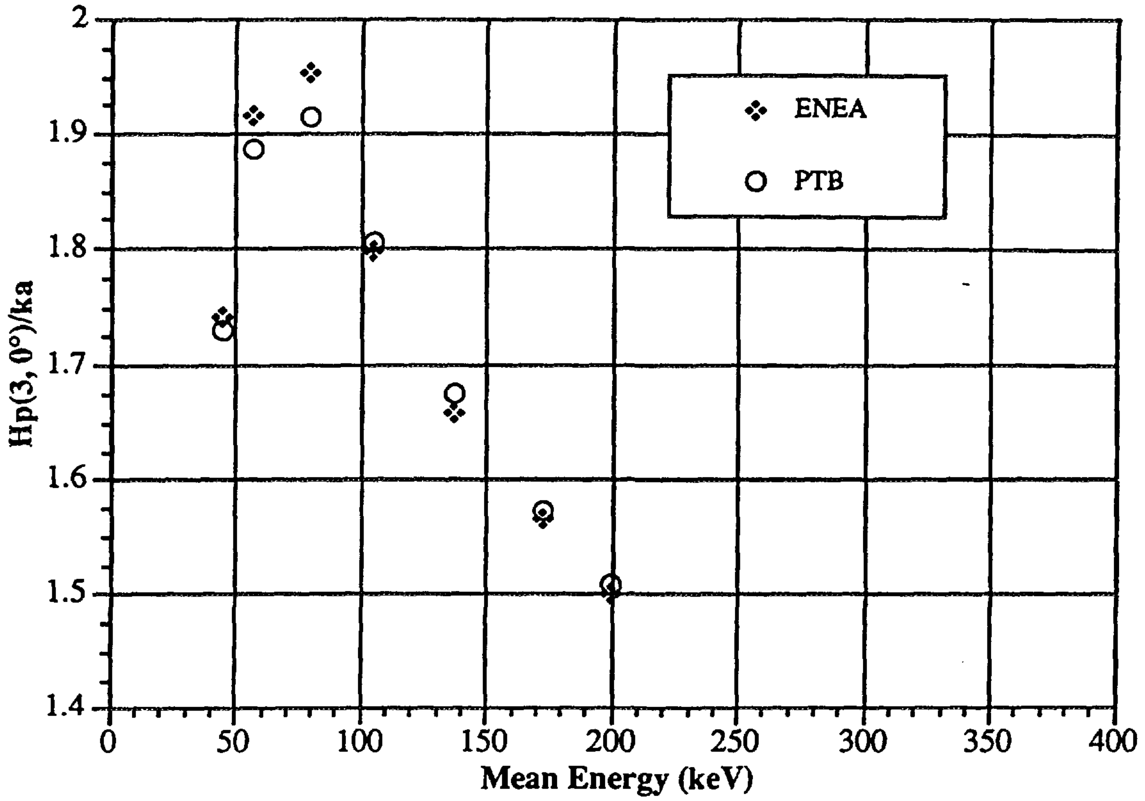

Fig. 16: Wide Spectrum Series: Hp(10,0°)/ka for PMMA slab phantom.

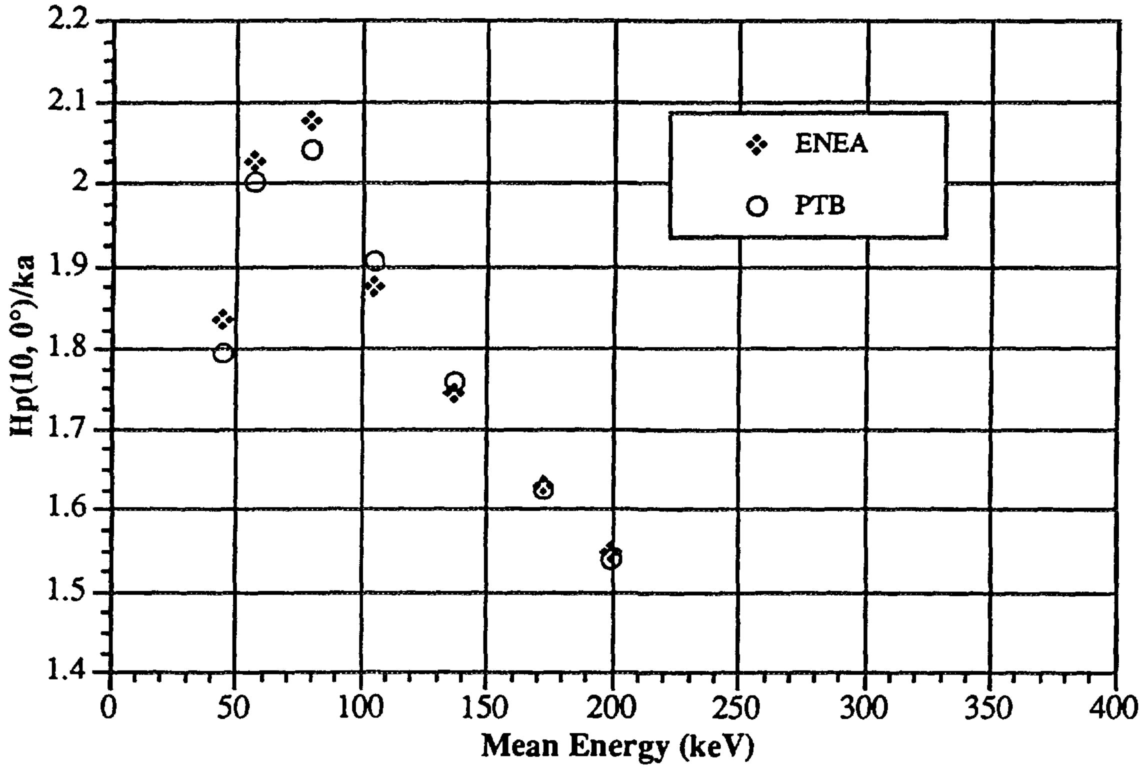

Fig. 17: Narrow Spectrum Series: Hp(0.07,0°)/ka for PMMA slab phantom.

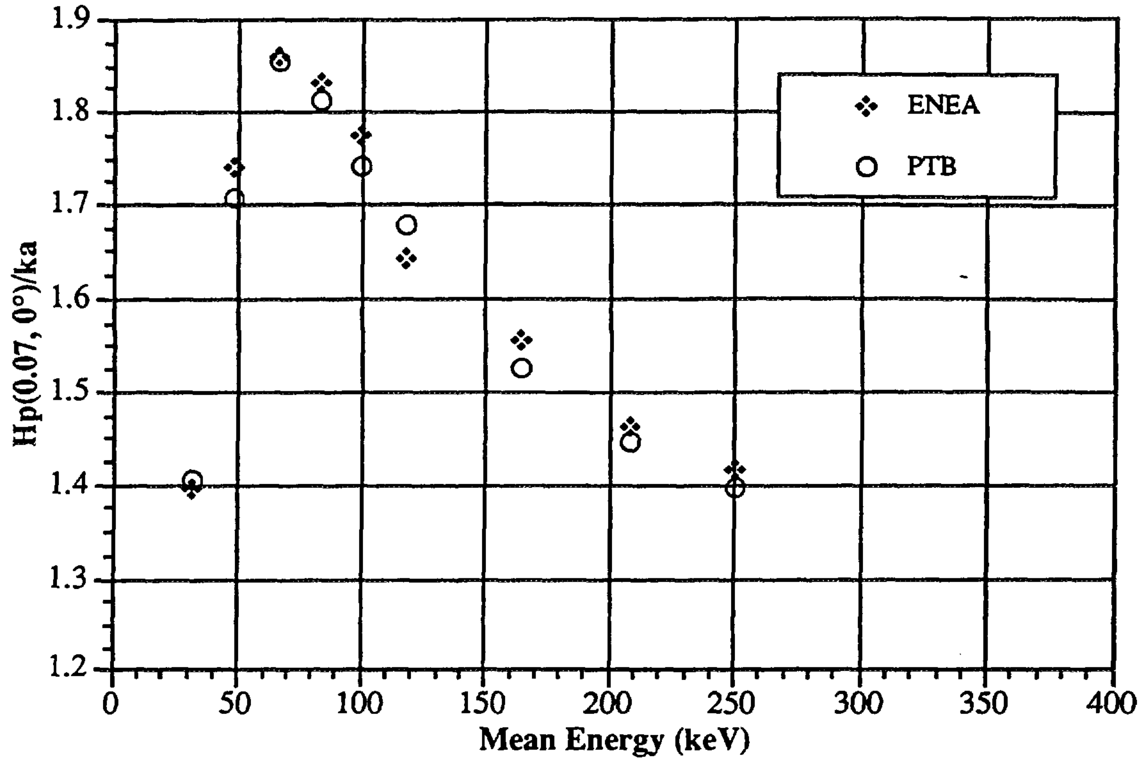

Fig. 18: Narrow Spectrum Series: Hp(0.07,0°)/ka for PMMA slab phantom.

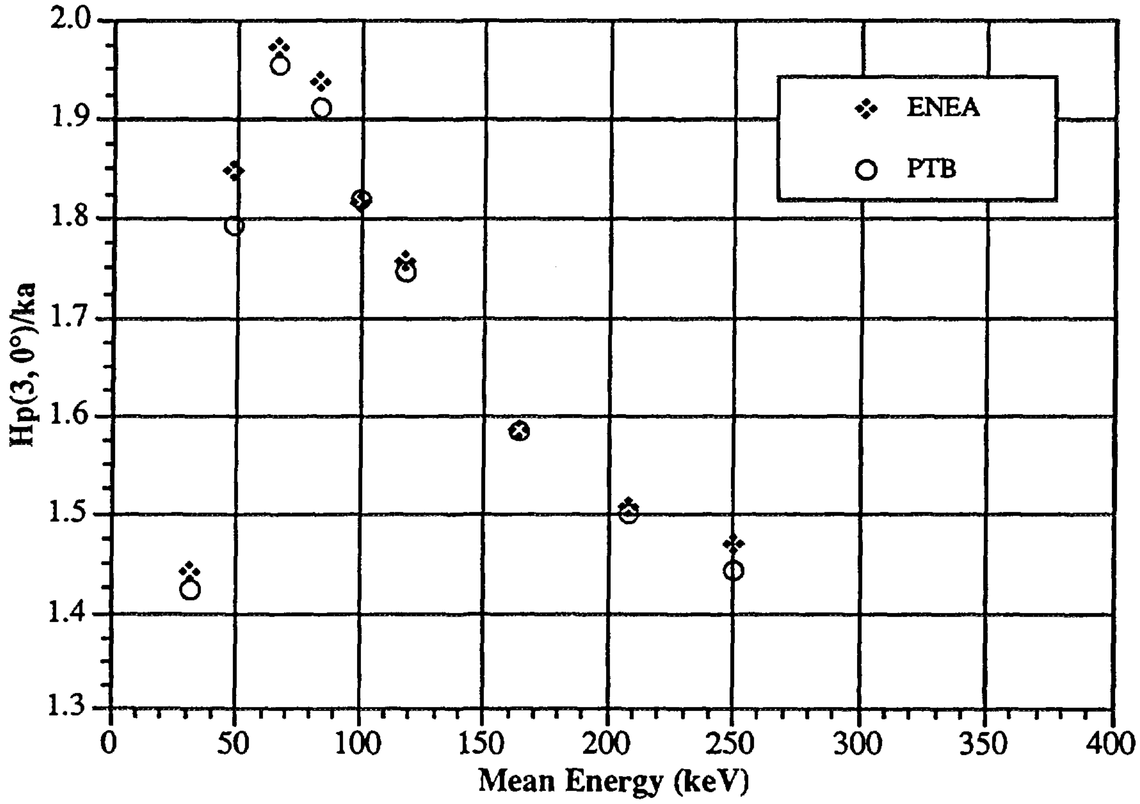

Fig. 19: Narrow Spectrum Series: Hp(10,0°)/ka for PMMA slab phantom.

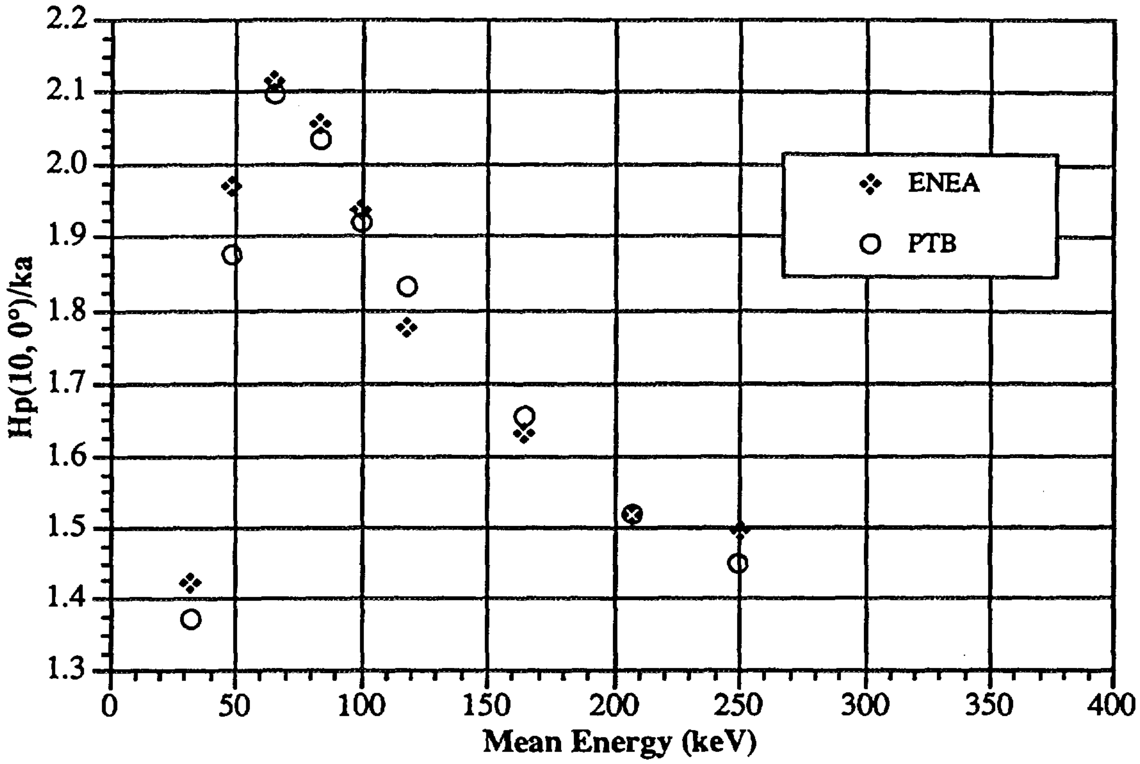

In Tab. IX, X, XI and XII the complete set of the results for normally incident beams is presented at 0.07, 0.1, 3 and 10 mm depths in the water filled PMMA phantom.

Tab. IX: Hp(0.07,0°)/ka values for water in PMMA slab phantom.

Depth =0.07 mm Hp(d,0°)/ka			
Water in PMMA			
Wide Spectrum Series		Narrow Spectrum Series	
Spectrum	ENEA	Spectrum	ENEA
L1 - 60 kV	1.526	S1 - 40 kV	1.290
L2 - 80 kV	1.667	S2 - 60 kV	1.598
L3 - 110 kV	1.726	S3 - 80 kV	1.716
L4 - 150 kV	1.638	S4 - 100 kV	1.733
L5 - 200 kV	1.548	S5 - 120 kV	1.697
L6 - 250 kV	1.485	S6 - 150 kV	1.599
L7 - 300 kV	1.449	S7 - 200 kV	1.505
		S8 - 250 kV	1.442
		S9 - 300 kV	1.393

Tab. X: Hp(0.1,0°)/ka values for water in PMMA slab phantom.

Depth =0.1 mm Hp(d,0°)/ka			
Water in PMMA			
Wide Spectrum Series		Narrow Spectrum Series	
Spectrum	ENEA	Spectrum	ENEA
L1 - 60 kV	1.531	S1 - 40 kV	1.290
L2 - 80 kV	1.672	S2 - 60 kV	1.605
L3 - 110 kV	1.786	S3 - 80 kV	1.712
L4 - 150 kV	1.640	S4 - 100 kV	1.743
L5 - 200 kV	1.547	S5 - 120 kV	1.675
L6 - 250 kV	1.486	S6 - 150 kV	1.602
L7 - 300 kV	1.448	S7 - 200 kV	1.508
		S8 - 250 kV	1.440
		S9 - 300 kV	1.390

Tab. XI: Hp(3,0°)/ka values for water in PMMA slab phantom.

Depth =3 mm Hp(d,0°)/ka			
Water in PMMA			
Wide Spectrum Series		Narrow Spectrum Series	
Spectrum	Hp/ka	Spectrum	Hp/ka
L1 - 60 kV	1.598	S1 - 40 kV	1.287
L2 - 80 kV	1.719	S2 - 60 kV	1.634
L3 - 110 kV	1.825	S3 - 80 kV	1.814
L4 - 150 kV	1.719	S4 - 100 kV	1.845
L5 - 200 kV	1.609	S5 - 120 kV	1.746
L6 - 250 kV	1.516	S6 - 150 kV	1.689
L7 - 300 kV	1.479	S7 - 200 kV	1.553
		S8 - 250 kV	1.462
		S9 - 300 kV	1.424

Tab. XII: Hp(10,0°)/ka values for water in PMMA slab phantom.

Depth =10 mm Hp(d,0°)/ka			
Water in PMMA			
Wide Spectrum Series		Narrow Spectrum Series	
Spectrum	ENEA	Spectrum	ENEA
L1 - 60 kV	1.554	S1 - 40 kV	1.259
L2 - 80 kV	1.768	S2 - 60 kV	1.619
L3 - 110 kV	1.885	S3 - 80 kV	1.881
L4 - 150 kV	1.702	S4 - 100 kV	1.839
L5 - 200 kV	1.671	S5 - 120 kV	1.754
L6 - 250 kV	1.545	S6 - 150 kV	1.673
L7 - 300 kV	1.483	S7 - 200 kV	1.583
		S8 - 250 kV	1.483
		S9 - 300 kV	1.423

The two practical materials' Hp/ka values for the two ISO series were compared (see Figures 20-25): a behaviour similar to that of the monoenergetic photons was obtained.

Fig. 20: Wide Spectrum Series:
Hp(0.07,0°)/ka comparison for PMMA and water in PMMA phantom.

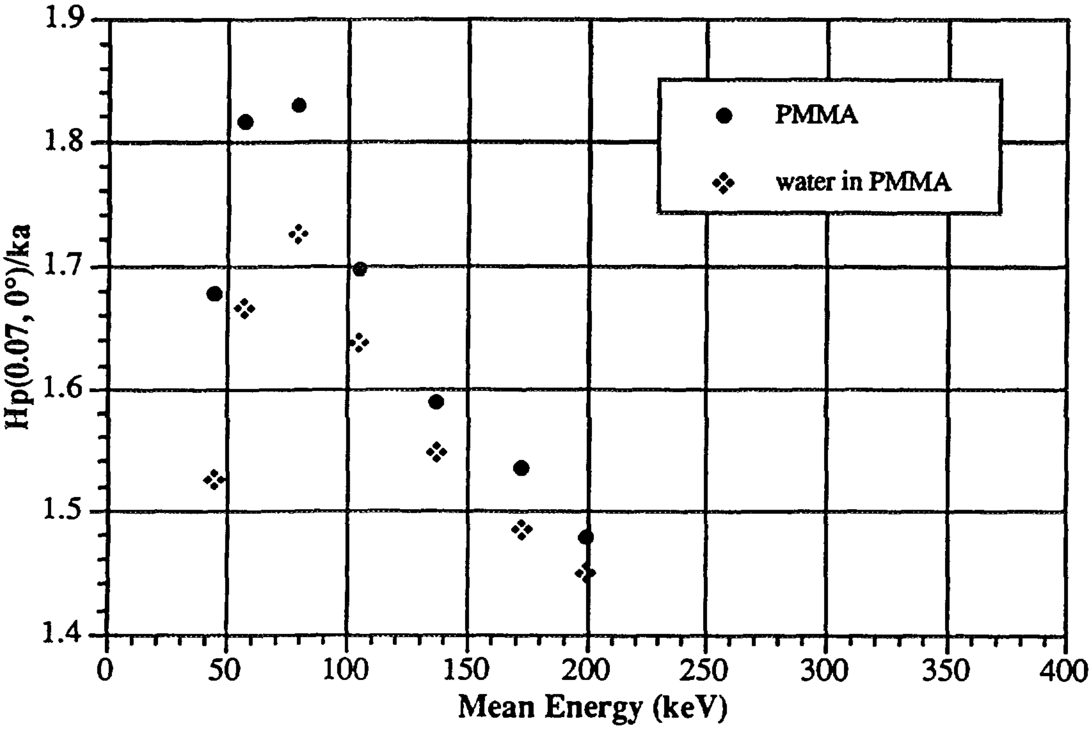

Fig. 21: Wide Spectrum Series:
Hp(3,0°)/ka comparison for PMMA and water in PMMA phantom.

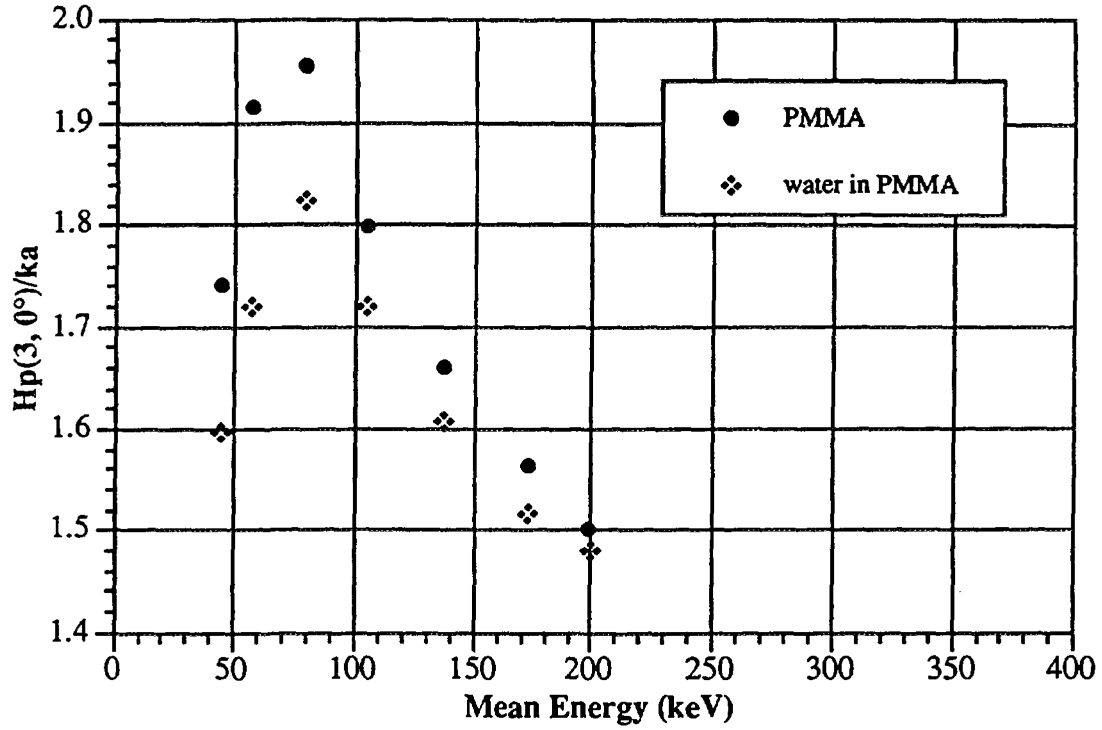

Fig. 22: Wide Spectrum Series:
Hp(10,0°)/ka comparison for PMMA and water in PMMA phantom.

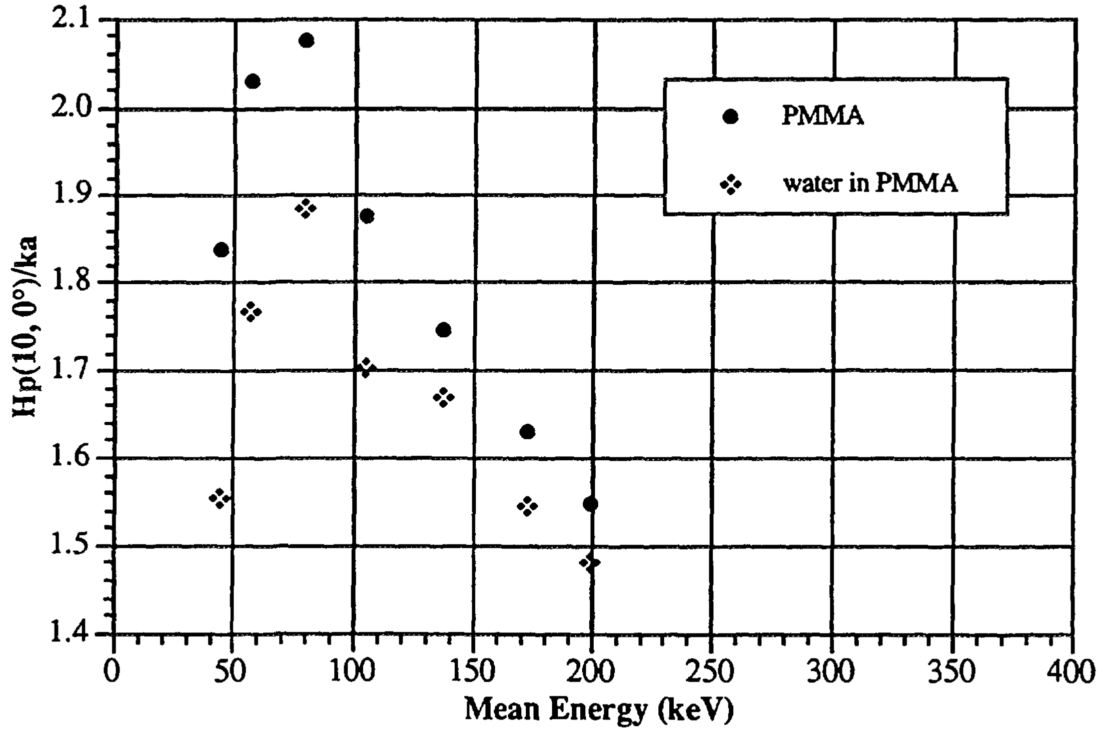

Fig. 23: Narrow Spectrum Series:
Hp(0.07,0°)/ka comparison for PMMA and water in PMMA phantom.

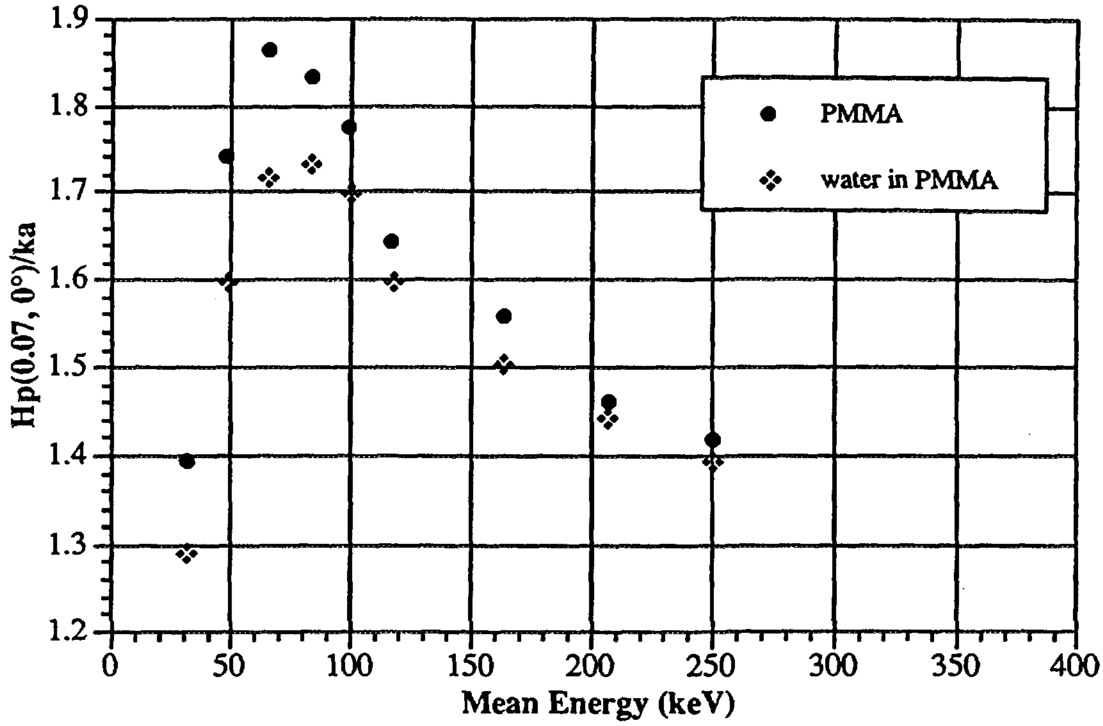

Fig. 24: Narrow Spectrum Series:
Hp(3,0°)/ka comparison for PMMA and water in PMMA phantom.

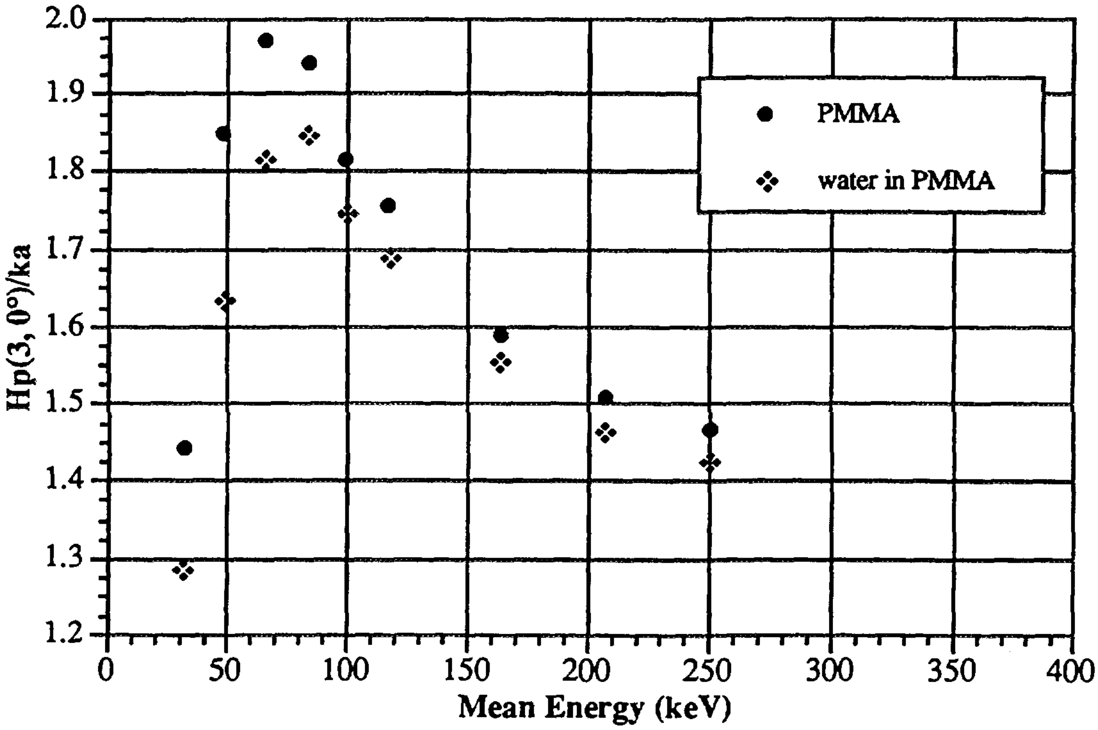

Fig. 25: Narrow Spectrum Series:
Hp(10,0°)/ka comparison for PMMA and water in PMMA phantom.

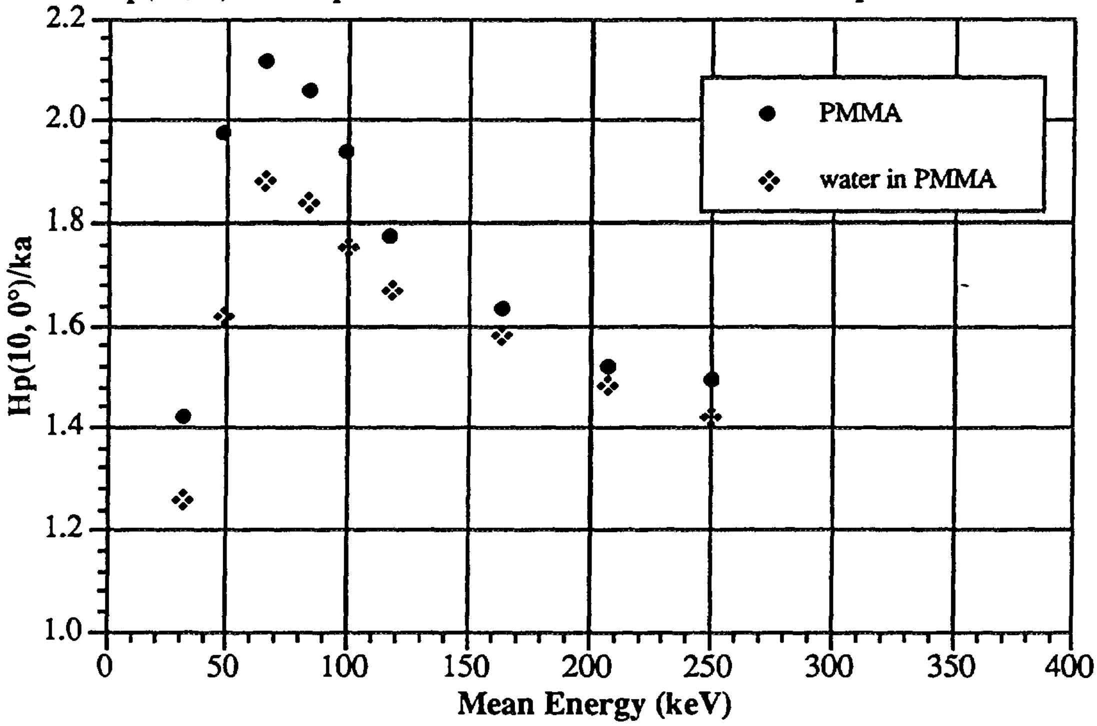

A series of comparisons were carried out between the set of data obtained for the previously discussed monoenergetic beams and the two ISO Series. For the spectra the data were plotted as a function of beam mean energy. Figures 26, 27, 28 show the comparison for the Narrow Series, that demonstrates that the mean energy of the X-ray beam is well representative of its behaviour so that a first good approximation is to use the conversion factors for monoenergetic photons of energy corresponding to the spectrum mean value.

Fig. 26: Comparison Narrow Spectrum Series - monoenergetic beams.

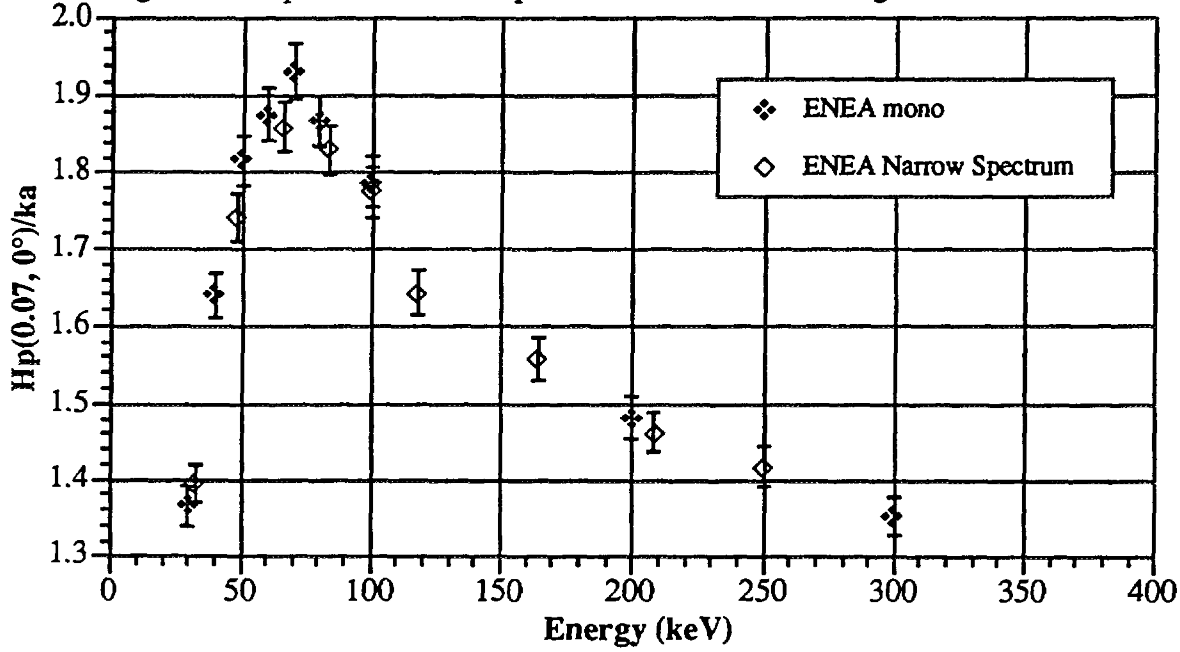

Fig. 27 Comparison Narrow Spectrum Series - monoenergetic beams.

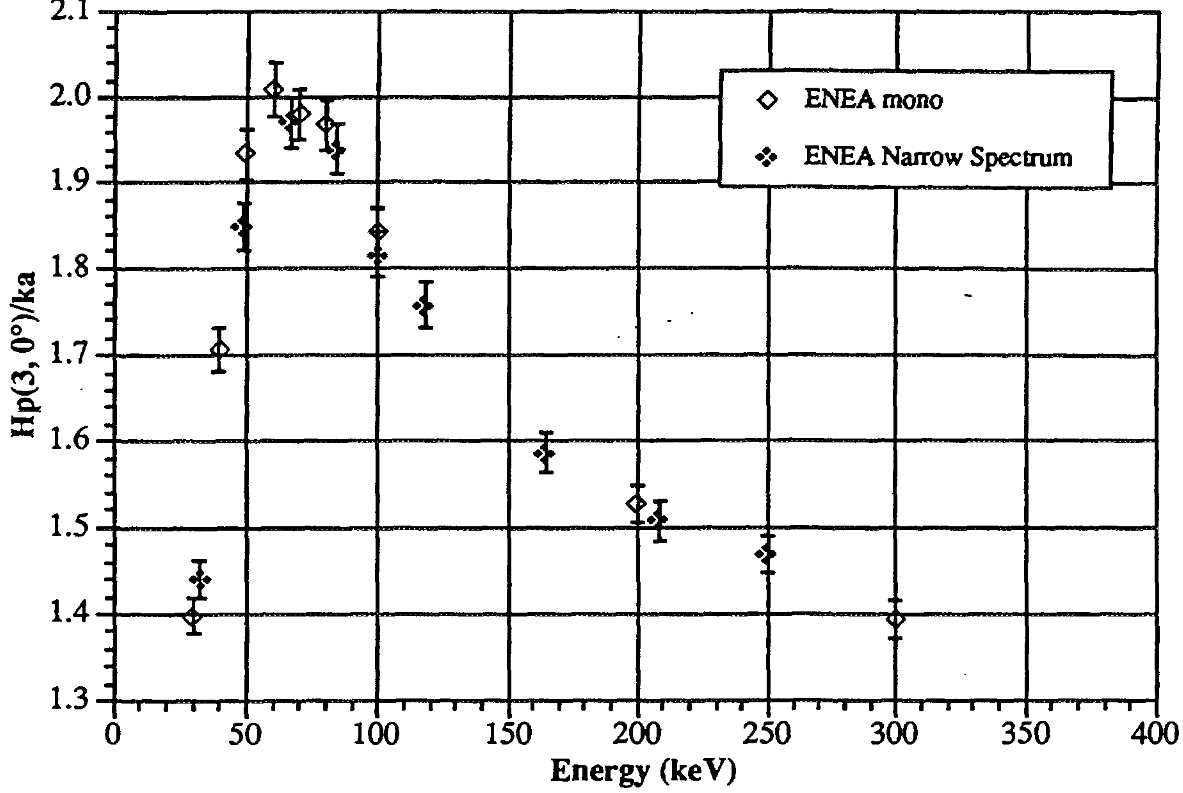

Fig. 28: Comparison Narrow Spectrum Series - monoenergetic beams.

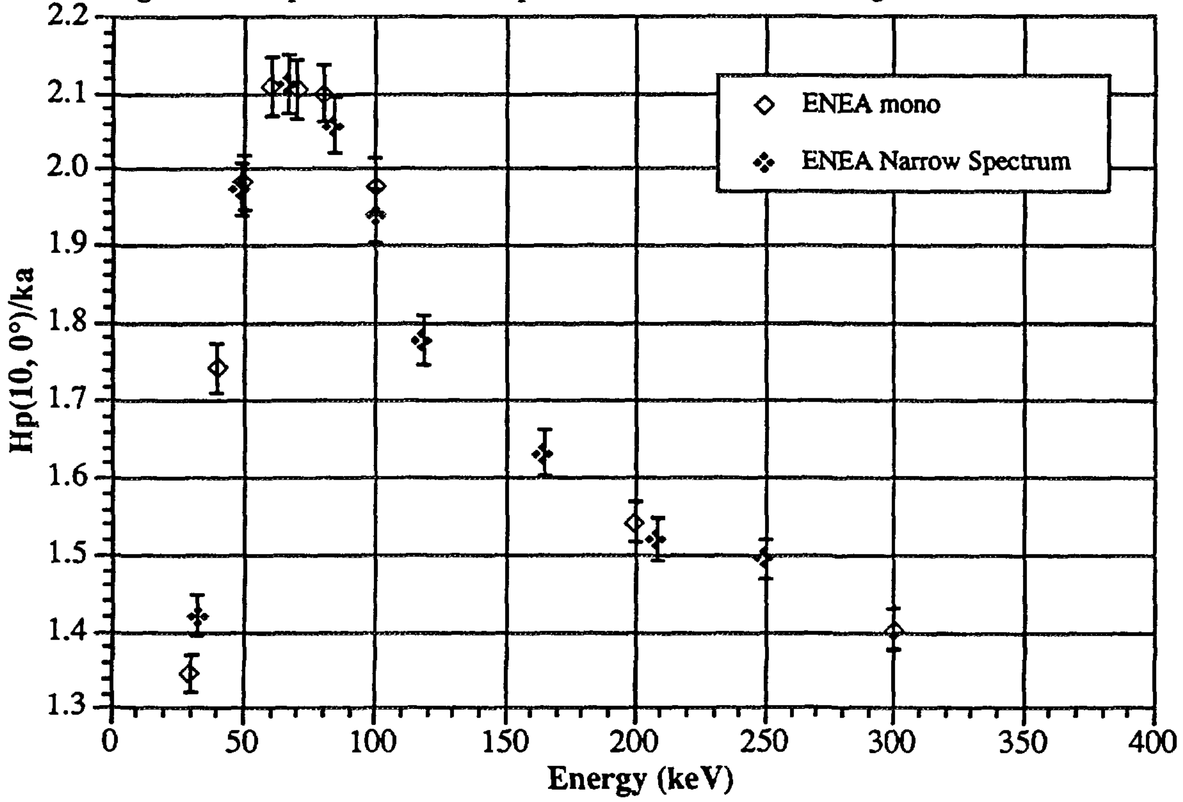

3.2-B Oblique incidence beams

The investigations at 45°, 60° as well as 75° incident angles were carried out only for the PMMA material.

Tables XIII-XVI show the Hp(d)/ka calculated at the four depths for the three investigated incident angles.

Tab. XIII: Hp(0.07,α)/ka values calculated at 45°, 60° and 75° incident angle for Wide and Narrow spectrum series.

PMMA Depth =0.07 mm Hp(d;α)/ka					
Wide Spectrum Series					
Spectrum	**Tube Voltage**	**Mean Energy**	**α=45°**	**α=60°**	**α=75°**
L1	60 kV	45.2	1.595	1.487	1.327
L2	80 kV	57.1	1.712	1.613	1.422
L3	110 kV	79.5	1.729	1.679	1.489
L4	150 kV	105.1	1.658	1.604	1.488
L5	200 kV	137.9	1.557	1.528	1.476
L6	250 kV	173.6	1.488	1.468	1.441
L7	300 kV	199.9	1.449	1.448	1.378
Narrow Spectrum Series					
S1	40 kV	32.6	1.348	1.292	1.183
S2	60 kV	48.6	1.644	1.551	1.370
S3	80 kV	66.2	1.778	1.684	1.482
S4	100 kV	83.7	1.743	1.704	1.548
S5	120 kV	100.2	1.669	1.632	1.530
S6	150 kV	118	1.621	1.574	1.466
S7	200 kV	164.6	1.504	1.506	1.401
S8	250 kV	208.2	1.474	1.438	1.376
S9	300 kV	250.2	1.4198	1.401	1.358

Tab. XIV: Hp(0.1,α)/ka values calculated at 45°, 60° and 75° incident angle.

PMMA Depth =0.1 mm Hp(d;α)/ka					
Wide Spectrum Series					
Spectrum	Tube Voltage	Mean Energy	α=45°	α=60°	α=75°
L1	60 kV	45.2	1.575	1.493	1.326
L2	80 kV	57.1	1.754	1.620	1.418
L3	110 kV	79.5	1.727	1.697	1.495
L4	150 kV	105.1	1.664	1.593	1.467
L5	200 kV	137.9	1.565	1.532	1.451
L6	250 kV	173.6	1.492	1.467	1.397
L7	300 kV	199.9	1.450	1.448	1.377
Narrow Spectrum Series					
S1	40 kV	32.6	1.350	1.294	1.174
S2	60 kV	48.6	1.641	1.547	1.365
S3	80 kV	66.2	1.772	1.686	1.482
S4	100 kV	83.7	1.742	1.709	1.534
S5	120 kV	100.2	1.675	1.637	1.498
S6	150 kV	118	1.621	1.568	1.465
S7	200 kV	164.6	1.508	1.502	1.424
S8	250 kV	208.2	1.4698	1.438	1.377
S9	300 kV	250.2	1.414	1.398	1.355

Tab. XV: Hp(10,α)/ka values calculated at 45°, 60° and 75° incident angle.

PMMA Depth =3 mm Hp(d;α)/ka					
Wide Spectrum Series					
Spectrum	Tube Voltage	Mean Energy	α=45°	α=60°	α=75°
L1	60 kV	45.2	1.636	1.488	1.190
L2	80 kV	57.1	1.777	1.650	1.329
L3	110 kV	79.5	1.8498	1.678	1.388
L4	150 kV	105.1	1.703	1.607	1.394
L5	200 kV	137.9	1.639	1.509	1.344
L6	250 kV	173.6	1.533	1.479	1.325
L7	300 kV	199.9	1.4896	1.460	1.291
Narrow Spectrum Series					
S1	40 kV	32.6	1.368	1.226	0.960
S2	60 kV	48.6	1.716	1.561	1.242
S3	80 kV	66.2	1.838	1.696	1.380
S4	100 kV	83.7	1.817	1.685	1.434
S5	120 kV	100.2	1.742	1.644	1.378
S6	150 kV	118	1.665	1.578	1.369
S7	200 kV	164.6	1.553	1.488	1.3196
S8	250 kV	208.2	1.489	1.454	1.281
S9	300 kV	250.2	1.441	1.422	1.281

Tab. XVI: Hp(10,α)/ka values calculated at 45°, 60° and 75° incident angle.

PMMA Depth =10 mm Hp(d;α)/ka					
Wide Spectrum Series					
Spectrum	**Tube Voltage**	**Mean Energy**	**α=45°**	**α=60°**	**α=75°**
L1	60 kV	45.2	1.620	1.368	0.873
L2	80 kV	57.1	1.7999	1.556	1.047
L3	110 kV	79.5	1.843	1.596	1.090
L4	150 kV	105.1	1.714	1.513	1.105
L5	200 kV	137.9	1.603	1.438	1.0595
L6	250 kV	173.6	1.507	1.395	1.041
L7	300 kV	199.9	1.464	1.425	1.037
Narrow Spectrum Series					
S1	40 kV	32.6	1.235	1.013	0.577
S2	60 kV	48.6	1.722	1.443	0.955
S3	80 kV	66.2	1.880	1.627	1.099
S4	100 kV	83.7	1.858	1.596	1.093
S5	120 kV	100.2	1.770	1.546	1.121
S6	150 kV	118	1.684	1.482	1.093
S7	200 kV	164.6	1.541	1.376	1.036
S8	250 kV	208.2	1.455	1.340	1.039
S9	300 kV	250.2	1.401	1.327	1.032

A very satisfactory internal agreement was obtained again between ISO beams' values and monoenergetic photon values obtained at ENEA for 75° incident angle, that is to confirm that from the practical point of view the conversion coefficients calculated for the spectrum mean energy can be used as a good estimate of the conversion factors for the whole spectrum (see figures 29, 30 and 31).

Fig. 29: Hp(0.07,75°)/ka comparison for monoenergetic beams - Narrow spectrum.

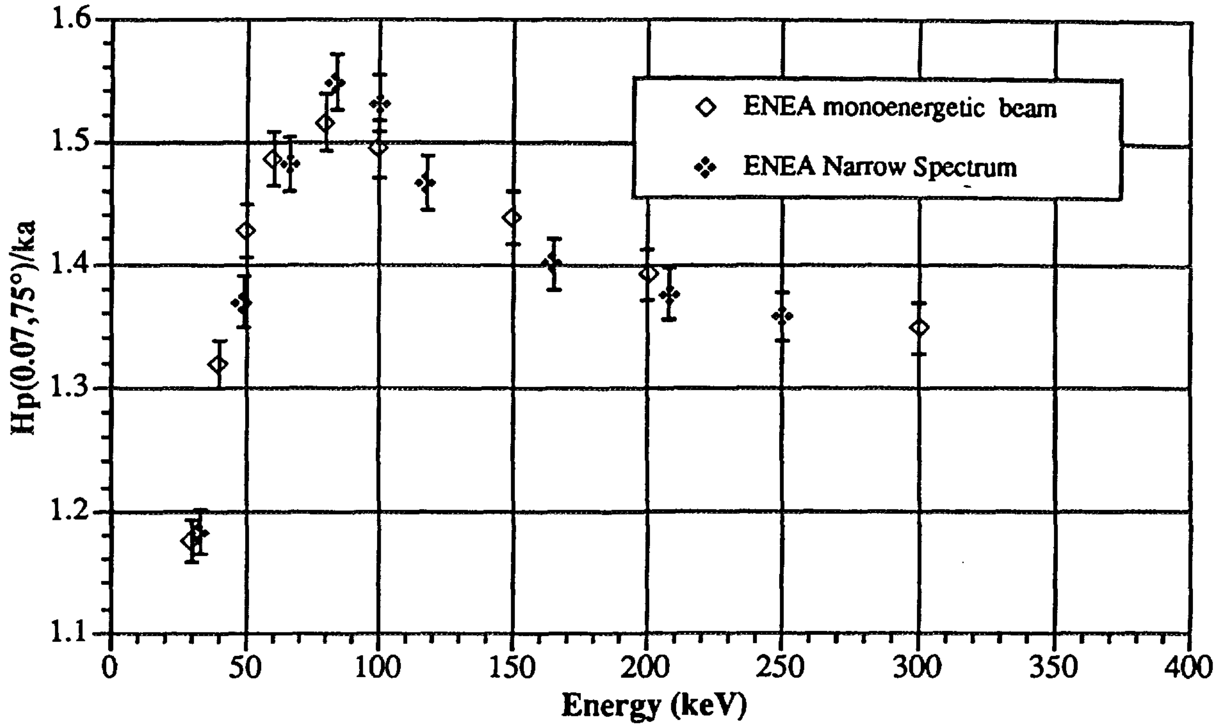

Fig. 30: Hp(3,75°)/ka comparison for monoenergetic beams and Narrow spectrum.

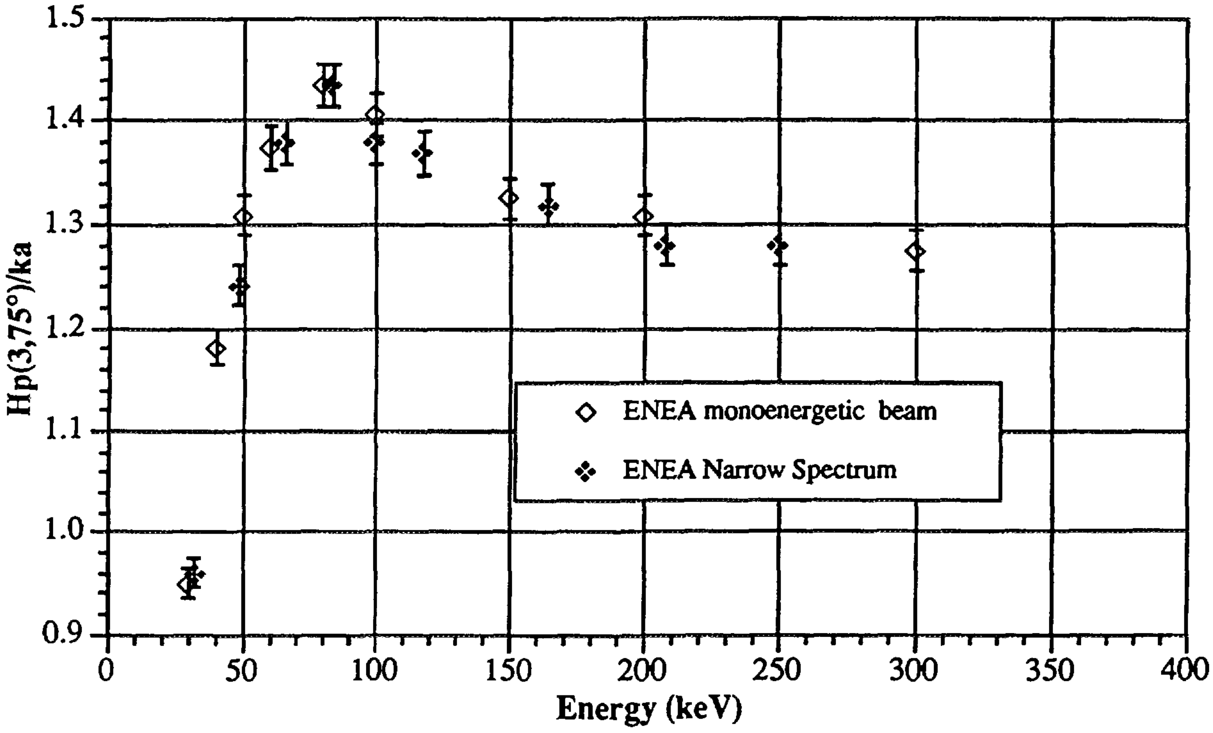

Fig. 31: Hp(10,75°)/ka comparison for monoenergetic beams and Narrow spectrum.

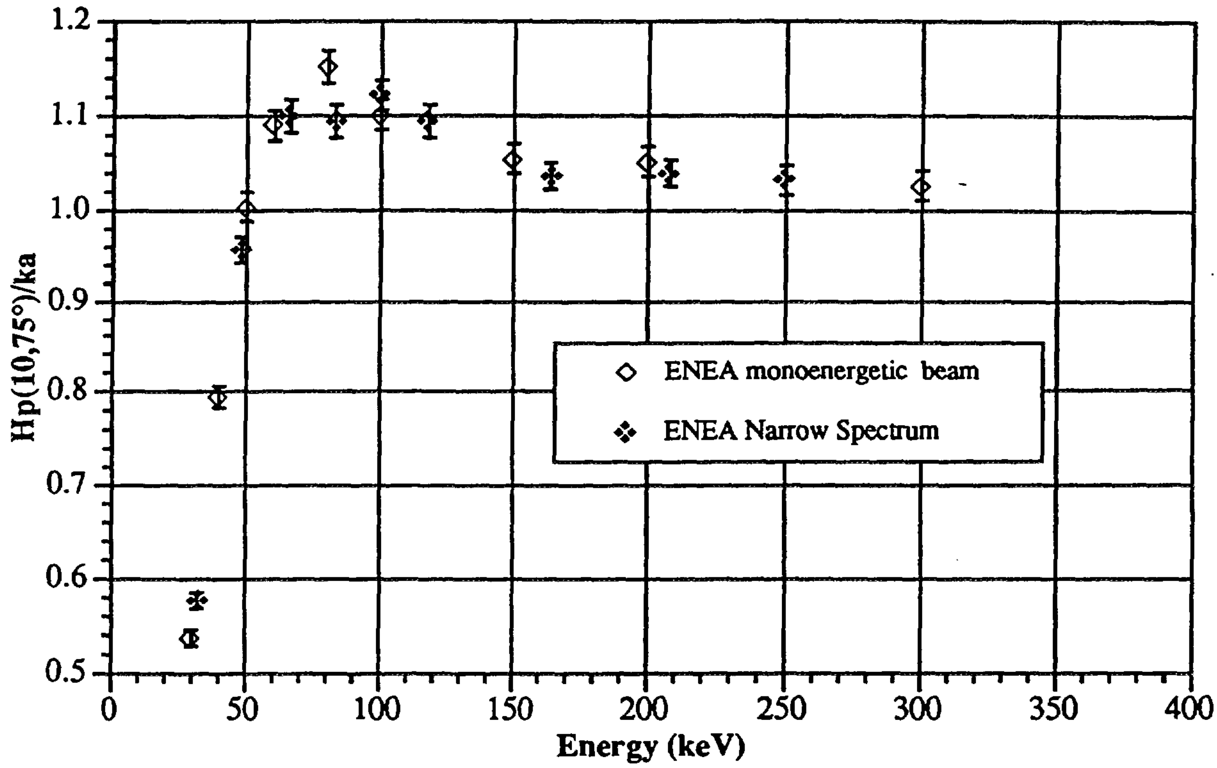

4. CONCLUSIONS

The studies on the practical calibration phantoms have been carried out for a variety of monochromatic photon energies and ISO X-ray reference Series in the energy domain from 20 keV to 1 MeV. They demonstrated that the ISO recommended water filled slab phantom is a better substitute of the ICRU theoretical one than the PMMA slab phantom, originally proposed by ICRU. The values of the personal dose equivalent at the three depths 0.07, 3 and 10 mm are very close to those calculated for the ICRU theoretical slab, so that, for practical purposes, one could directly use these values, together with the practical slab without introducing correction factors. The phantom is easy to be made so that this new proposal seems to fulfil the requirements of an easy routine calibration procedure to be applied in agreement with the definitions reported in the ICRU documents.

Besides the calculation of normal incidence values, the studies were also aimed to investigating the angular dependence of the conversion coefficients Hp(d,α)/ka for 45°, 60° and 75° angles that are important to be known, dealing with non-normally incident practical fields, to guarantee an isodirectional response (i.e. the response has to be very close to Hp(d,α)) of the dosemeter for personal dosimetry purposes.

Furthermore the data were compared with independent calculations by Grosswendt, obtaining a satisfactory agreement as a function of energy .

On the other hand, as far as the routine calibration practice is concerned, following the International Recommendations (ICRU) it has to be pointed out that in principle both PMMA and water slab phantoms can be employed, simply taking into account (with an appropriate correction factor) the different backscatter characteristics of the two practical phantoms compared with the ICRU theoretical one and applying the conversion factor from air kerma to personal dose equivalent Hp value as defined on the theoretical 4-element tissue slab.
The detailed physical comparison of the two proposed phantoms, as shown in the present report, took into account also the ICRU operational quantities as defined within the practical investigated phantoms. This analysis allowed some more exhaustive considerations.

The set of data shown in the present report can contribute in Italy to provide guidance towards the adoption of the new criteria for the photon personal dosemeter calibration according to the ICRU recommendations.

References

/1/ ICRU Report 39 "Determination of Dose Equivalents Resulting from External Radiation sources.", Bethesda - Maryland (1985).
/2/ Gualdrini G., Lembo L., Monteventi F. and Padoani F. "Monte Carlo calculation of Field Parameters for the ICRU Sphere with Reference Photon Beams." Rad. Prot. Dosim. 46, 5-13 (1993).
3/ Gualdrini G. F. " Field Parameters and Operational Quantities for the ICRU sphere with Reference Photon Beams. PART 1° Monte Carlo calculation of angular distribution of backscatter factors. ENEA/RT/AMB/92/12.
/4/ Gualdrini G. F. , Padoani F. and Morelli B. "Field Parameters and Operational Quantities for the ICRU sphere with Reference Photon Beams. PART 2° Monte Carlo calculation of backscattered spectra and backscattered mean energy angular distribution." ENEA/RT/AMB/92/13.
/5/ Gualdrini G.F., Monteventi F. and Sermenghi I. " Field Parameters and Operational Quantities for the ICRU sphere with Reference Photon Beams. PART 3° Experimental and computational analyses on the tissue substitute material RS-1" ENEA/RT/AMB/92/24
/6/ Morelli B. and Gualdrini G.F. Monteventi F." Field Parameters and Operational Quantities for the ICRU sphere with Reference Photon Beams. PART 4°. Monte Carlo and Experimental Evaluation of Angular Dependence of Dose Equivalent Quantities ENEA/RT/AMB/94/19.
/7/ Gualdrini F. and Morelli B. "Studies on the Field Homogeneity Area on Tissue Equivalent Slab Phantoms for ISO X-Ray Reference Beams", forthcoming ENEA report.
/8/ ICRU Report 47 "Measurement of Dose Equivalents from External Photon and Electron Radiations". Bethesda Maryland(1992).
/9/ ICRU Report 51 "Quantities and Units in Radiation Protection Dosimetry". Bethesda Maryland (1993).
/10/ Bohm J. "Minutes of the ISO/TC85/SC2/WG2 Meeting in London on 25-27 October 1993", PTB Braunschweig, November 1993.
/11/ Grosswendt B. "The Angular Dependence and Irradiation Geometry Factor for the Dose Equivalent for Photons in Slab Phantoms of Tissue Equivalent Material and PMMA." Rad. Prot. Dosim. 35, 221-235 (1991).

/12/ "MCNP: A General Monte Carlo Code for Neutron and Photon Transport". LA-7396-M rev. Sept 2 (1986).
/13/ Hubbell J. H., et al. " Atomic Form Factors, Incoherent Scattering Functions, and Photon Scattering Cross Sections." J. Phys. Chem. Ref. Data 4, 471 (1975).
/14/ Laitano F., Toni M.P. et al. " Energy Distributions and B.I.P.M. References Filtered X-Radiation", ENEA Report, December 1990.

Edito dall' ENEA
Funzione Centrale Relazioni
Lungotevere Grande Ammiraglio Thaon di Revel, 76 - 00196 Roma
Stampa: RES-Centro Stampa Tecnografico - C. R. Frascati

Finito di stampare nel mese di ottobre 1996